IDENTIFICATION OF HOST FACTORS FOR DEVELOPING ANTIVIRAL STRATEGIES AGAINST INFLUENZA VIRUS

By

SUNIL MORE

Bachelor of Veterinary Sciences and Animal Husbandry
Maharashtra Animal and Fishery Sciences University
Nagpur, Maharashtra
2007

Master of Veterinary Science
in
Animal Genetics and Breeding
Maharashtra Animal and Fishery Sciences University
Nagpur, Maharashtra
2009

Submitted to the Faculty of the
Graduate College of the
Oklahoma State University
in partial fulfillment of
the requirements for
the Degree of
DOCTOR OF PHILOSOPHY
May, 2016

IDENTIFICATION OF HOST FACTORS FOR DEVELOPING ANTIVIRAL STRATEGIES AGAINST INFLUENZA VIRUS

Dissertation Approved:

Dr. Lin Liu

Dissertation Adviser

Dr. Anthony Confer

Dr. Tom Oomens

Dr. Glenn Zhang

ACKNOWLEDGEMENTS

I wish to express my appreciation and deep gratitude to my major advisor Dr. Lin Liu. His constant support during the course of study is highly appreciated. I thank him for the constant encouragement, his emphasis on clear scientific communication, and critical suggestions. His confidence in me made me work hard and become competitive. I wish to thank the members of my doctoral advisory committee – Dr. Anthony Confer, Dr. Tom Oomens and Dr. Glen Zhang – for their encouragement and expert advice during the research. To have such experts in the committee is an honor, and I sincerely thank them for their support, patience and faith in me over the past five years. I would also like to thank Dr. Keith Bailey for his help and mentorship in reading histopathology slides related to mice studies.

I would like to thank all the past and present members of Dr. Liu's lab. It has been a pleasure to work with them, and I have learnt so much from them along the way. I have greatly enjoyed my teaching assistant job in Dog Anatomy during this time. I thank all the instructors and fellow TA's including Dr. Larry Stein, Dr. Alastair Watson, Dr. Pradyumna Baviskar, Dr. Girija Regmi and Dr. Kalyani Ektate, for their guidance and inspiration. I would also like to thank Christopher Pivinski for his help in the dissection labs. I would like to express my sincere gratitude to Center for Veterinary Health Sciences for supporting my research and also to all the staff and non-staff members at Center for Veterinary Health Sciences. I take this opportunity to thank all my friends including my fellow graduate students for their encouragements and also for keeping me motivated.

Last, but certainly not least, I thank my mother, brother and sister and my wife Ankita for their support and love. I sincerely appreciate their endless patience and encouragement when it was most required. It is their faith in me which help me make this achievement possible. This one is dedicated to my belated father. We miss you!

Name: SUNIL MORE

Date of Degree: MAY, 6TH 2016

Title of Study: DEVELOPING ANTIVIRAL STRATEGIES AGAINST INFLUENZA VIRUS USING HOST FACTORS

Major Field: VETERINARY BIOMEDICAL SCIENCE

Abstract:

The Wnt/β-catenin signaling is an essential pathway involved in cell cycle control. Dysregulation of Wnt/β-catenin signaling pathway has been reported during viral infections. In this study, we examined the effect of modulating Wnt/β-catenin signaling during influenza virus infection. The activation of the Wnt/β-catenin pathway with Wnt3a increased mRNA expression of influenza virus genes *in vitro* in mouse lung epithelial E10 cells and *in vivo* in the lungs of mice infected with influenza virus A/Puerto Rico/8/34. However, inhibition of Wnt/β-catenin signaling with iCRT14 reduced virus titer and viral gene expression in human lung epithelial A549 cells and viral replication in primary mouse alveolar epithelial cells infected with influenza virus A/Puerto Rico/8/34 and A/WSN/1933. iCRT14 acts at the early stage of virus replication and its anti-viral activity is independent of interferon response. Treatment with iCRT14 inhibited the expression of viral genes (vRNA, cRNA and mRNA) evaluated. Intraperitoneal administration of iCRT14 reduced viral load, improved clinical symptoms, and partially protected mice from influenza virus infection.

Long non-coding RNAs (lncRNAs) are a new arm of gene regulatory mechanism as discovered by sequencing techniques and functional studies. There are only few studies on lncRNAs as related to gene expression regulation and anti-viral activity during influenza virus infection. Using RNA sequencing analysis, we found that 1,912 lncRNAs were significantly changed in human lung epithelial A549 cells infected with influenza A/Puerto Rico/8/34 along with high enrichment of type I interferon signaling and cellular response genes based on Go ontology. Seven selected up-regulated lncRNAs were verified by real-time PCR and were also induced by other two influenza H1N1 virus strains (A/WSN/1933 and A/Oklahoma/3052/09) and interferon β1. Knockdown of TAP1 and PSMB8 antisense RNA 1 (TAPSAR1) using lentiviral shRNA reduced the release of progeny influenza virus particles and inhibited viral protein synthesis but had no effects on viral mRNA level in single-cycle and multi-cycle infections. Knockdown of TAPSAR1 did not change the expression level of its neighboring gene PSMB8, but markedly reduced interferon gamma-induced protein 10 expression. Our study suggests that lncRNA TAPSAR1 could be a new host factor target for developing antiviral therapy against influenza virus infection.

TABLE OF CONTENTS

Chapter Page

I. INTRODUCTION 1

1.1 Influenza virus 1
1.2 Wnt signaling pathway 2
1.3 Long non-coding RNAs 3
1.4 Functions of lncRNAs 3
1.5 LncRNAs in innate and adaptive immune signaling 4
1.6 LncRNAs and influenza virus 5
1.7 Objectives of the study 5

II. MATERIALS AND METHODS 6

2.1 Cell culture 6
2.2 Isolation of primary mouse epithelial cells 6
2.3 Preparation of Wnt3a conditioned media 7
2.4 Influenza virus stocks 8
2.5 Virus infection of the cells 8
2.6 Immunofluorescence 8
2.7 Cell viability assay 9
2.8 RNA isolation and quantitative real-time PCR 9
2.9 Animal studies 12
2.10 Lactate dehydrogenase (LDH) assay and total protein measurement 12
2.11 Histopathological analyses 13
2.12 RNA sequencing and data analysis 13
2.13 Interferon treatment and lncRNA induction 14
2.14 Lentivirus shRNA vector construction 14
2.15 Lentivirus preparation and infection 15
2.16 Western blot analysis 16
2.15 Isolation of cytoplasmic and nuclear RNAs 17
2.16 Data analysis 17

III. RESULTS 18

3.1 Activation of Wnt/β-catenin signaling increases influenza virus replication 18
3.2 iCRT14 inhibits influenza virus infection 19
3.3 iCRT14 acts on early stage of influenza virus life cycle 21
3.4 iCRT14 reduces influenza virus RNA synthesis 22

3.5 Antiviral activity of iCRT14 is independent of interferon production 24
3.6 iCRT14 reduces influenza virus infection in primary alveolar epithelial cells 25
3.7 iCRT14 partially protects mice from a lethal dose of influenza virus challenge 27
3.8 iCRT14 attenuates clinical signs associated with a sublethal dose of influenza virus challenge 28
3.9 Effect of iCRT14 on lung histopathology of mice infected with a sub-lethal dose of A/PR/8/34 challenge 30
3.10 iCRT14 toxicity 33
3.11 LncRNAs are differentially expressed in influenza virus-infected A549 cells 33
3.12 GO pathway analysis of lncRNAs 38
3.13 Validation of RNA-seq results with qPCR 40
3.14 Effects of influenza virus strains on lncRNA expression 42
3.15 LncRNAs are induced by IFNβ1 44
3.16 Knockdown of lncRNAs using lentiviral shRNAs 45
3.17 Knockdown of TAPSAR1 reduces influenza virus replication 47
3.18 TAPSAR 1knockdown results in reduced influenza viral proteins synthesis and mRNAs 48
3.19 TAPSAR1 is localized in nucleus of A549 cells 51
3.20 Knockdown of TAPSAR1 does not affect its neighboring gene PSMB8 52
3.21 TAPSAR1 knockdown results in the reduction of IP10 54

IV. DISCUSSION 55

4.1 Influenza virus and host signaling pathways 55
4.2 Wnt signaling and influenza virus. 56
4.3 iCRT14 and interferon response 57
4.4 iCRT14 and vivo studies 57
4.4 RNA-seq experiment 58
4.6 LncRNA and viruses 59
4.7 Function of TAPSAR1 59
4.8 LncRNA location and neighbouring genes 60
4.9 IP10 and influenza virus infection 61

V. CONCLUSION 62

5.1 Wnt signaling inhibitor iCRT14 and influenza virus 62
5.2 ICRT14 protects mice from influenza virus infection 62
5.3 LncRNA and influenza virus 62
5.4 Effect of lncRNA TAPSAR1 on influenza virus replication 63

REFERENCES 64

LIST OF TABLES

Table Page

1. Real-time PCR primers 11
2. Oligos used for constructing lncRNA shRNAs 15
3. Histopathology of the lungs of mice infected with a sublethal dose of influenza virus.....32
4. Summary of RNA-seq data sets.....36
5. Interferon-stimulated antiviral genes 36
6. Selected lncRNAs and their properties.....37

LIST OF FIGURES

Figure Page

3.1 Wnt3a increases influenza virus gene expression....19
3.2 iCRT14 reduces influenza virus infection....20
3.3 Effect of iCRT14 on stages of the influenza virus life cycle....21
3.4 iCRT14 effect on influenza virus RNA synthesis....23
3.5 iCRT14-mediated inhibition of influenza virus RNA synthesis is independent of the IFN response....24
3.6 Effect of iCRT14 on influenza virus infection in primary mouse alveolar epithelial cells (AECs)....26
3.7 Effects of iCRT14 on weight loss and survival rate in mice challenged with a lethal dose of A/PR/8/34....27
3.8 Effect of iCRT14 on lung injury and inflammation of mice with a sub-lethal dose of A/PR/8/34 challenge....29
3.9 Histopathology of mice lungs with a sub-lethal dose of A/PR/8/34 and treated with iCRT14....31
3.10 lncRNAs are differentially regulated after influenza virus infection....35
3.11 GO pathway analysis of co-expressed mRNAs....39
3.12 Real-time PCR confirmation of RNA-seq results....41
3.13 LncRNA induction by different influenza viruses....43
3.14 Effect of IFNβ1 on lncRNA expression....44
3.15 Knockdown efficiency of lncRNA shRNAs....46
3.16 Effect of lncRNA knockdown on influenza virus replication....47
3.17 Effect of TAPSAR1 knockdown on influenza virus protein synthesis....49
3.18 Effect of TAPSAR1 knockdown on influenza virus mRNAs....50
3.19 Location of TAPSAR1 in A549 cells....51
3.20 Effect of TAPSAR1 knockdown on gene expression of PSMB8....53
3.21 Antiviral response gene profiles after TAPSAR1 knockdown....54

CHAPTER I

INTRODUCTION

1.1 Influenza virus

Influenza virus is a single stranded, negative sense RNA virus belonging to the *Orthomyxoviridae* family. It has 8 genome segments, which encode 10 - 12 different proteins (1). The replication mechanism of the virus is error-prone, resulting in mutations in the genome of the virus (2, 3). These changes lead to the development of antiviral drug resistance against most of the current antivirals drugs available in the market and is the reason for new influenza virus vaccines each season due to antigenic shift (4). Antigenic drift results from gradual point mutations in surface antigens during replication of the virus, whereas antigenic shift occurs due to genetic reassortment when two different influenza viruses infect the same cell. Antigenic shift causes the emergence of pandemic strains of virus, which can potentially infect huge populations of humans and animals (5).

Use of vaccine during the pandemics has many limitations such as lag time in vaccine production, efficacy of the vaccine in the population and access to the vaccine during pandemics (6). Thus, patient care depends upon the availability of effective antiviral drugs. However, emerging influenza viruses become resistant to the current antivirals because they target the viral proteins (7, 8). The FDA-approved drugs, adamantane and oseltamivir target M2 ion channel and neuraminidase, respectively. Several compounds targeting the virus polymerase complex are being developed for

anti-influenza virus drugs (9-12), but have the same limitation of drug resistance. Due to its small genome size, influenza virus is dependent on the host cell machinery for its replication from virus entry to exit from the host cells. Many host factors utilized by influenza virus have been identified at various stages of the virus life cycle (13, 14). Targeting these factors for developing antivirals can overcome the limitation of drug resistance of the current anti-influenza virus drugs.

1.2 Wnt signaling pathway

The Wnt/β-catenin signaling pathway plays an important role in cellular development and differentiation and has been implicated in developmental diseases and cancer (15). This pathway is activated by binding of Wnt ligands to the Frizzled receptor. In the absence of Wnt ligands, the central component, β-catenin is marked by ubiquitination for degradation via the destruction complex composed of adenomatous polyposis coli (APC), axin and glycogen synthase kinase 3β (GSK3β). When Wnt ligands are present, the complex is destabilized, leading to the accumulation and nuclear translocation of cytosolic β-catenin. In the nucleus, β-catenin interacts with the T cell factor/lymphoid enhancer binding factor 1 (TCF/LEF) transcription factor to activate Wnt target genes. iCRT14 is specific inhibitor of Wnt/β-catenin signaling which disrupts the direct interaction between β-catenin and TCF4/LEF1(16). This inhibitor also prevents the binding of TCF4 to DNA; however, iCRT14 does not affect non-canonical Wnt signaling and other pathways such as Hedgehog, JAK/STAT and notch signaling (16).

There are several studies regarding the interaction of the Wnt/β-catenin signaling pathway and viruses including human immunodeficiency virus (HIV) and hepatitis C virus (HCV). HIV's negative regulatory factor (Nef) protein interacts with β-catenin to inhibit Wnt/β-catenin signaling (17). The core protein and nonstructural NS5A protein of HCV activate the Wnt/β-catenin signaling pathway (18) (19). Kumar *et al.* has shown that activation of Wnt/β-catenin with lithium chloride (LiCl) reduces HIV propagation in peripheral mononuclear cells (20) and Narasipura *et al.* has reported that knock down of TCF4 or β-catenin enhanced HIV transcription (21). However, studies

on the role of Wnt/β-catenin signaling in influenza virus infection are very limited. In this study, we investigated the effect of Wnt/β-catenin signaling activation and inhibition on influenza virus infection.

1.3 Long-non coding RNAs

Only approximately 2% of human genome is used for protein-coding genes (22). Recent advances in sequencing technologies have enabled the discovery of vast portions of non-coding transcripts. Long non-coding RNAs (lncRNAs) are non-coding transcripts that have a length of > 200 nucleotides and do not encode any proteins. Although very few lncRNAs have been studied, lncRNAs play roles in development and diseases. LncRNA expression shows greater cell- and tissue-specificity than protein-coding genes (23, 24). The number of lncRNAs increases with developmental complexity (25), leading to the idea that lncRNAs play an important role in giving rise to the diversity of cell differentiation programs underlying development in multicellular organisms. Dysregulation of lncRNAs has been observed under many pathological conditions including respiratory diseases (26), cancers (27, 28) and heart diseases (29), indicating that abnormal expression of lncRNAs contributes to the development of pathophysiological conditions.

1.4 Function of lncRNAs

The functions of lncRNAs are diverse including chromatin remodeling, transcription and post transcription regulation, decoying, scaffolding, and microRNA sponging. Examples of epigenetic gene regulation by lncRNAs are X-inactive specific transcript (Xist) and HOX transcript antisense RNA (HOTAIR). They define epigenetic changes by interacting with various chromatin modifiers to alter their structure and in turn govern the accessibility of DNA to transcription factors and polymerase (27, 30). One example where lncRNA can directly interfere with polymerase II (Pol II) activity is the inhibition of the major coding transcript of dihydrofolate reductase (DHFR) (31). In dormant cells, an upstream minor promoter of DHFR produces a lncRNA that apparently interrupts

formation of the transcription preinitiation complex at the major promoter. Several lncRNAs act as RNA decoys. These lncRNAs titrate transcription factors away from their DNA targets by directly binding to them and thus suppress the transcription. LncRNA PANDA is one such example, which sequester nuclear transcription factor Y, alpha (NF-YA) away from its pro-apoptotic gene (32). At the post-transcriptional level, lncRNAs can function as microRNA target site decoys, titrating microRNA effector complexes away from their mRNA targets. For example, the tumor suppressor pseudogene PTENP1 sequesters miR-19b and miR-20a to regulate the target gene expression of these microRNAs (33). LncRNAs also act as a scaffold by binding specific combinations of regulatory proteins, enforcing a transcription silent state or contributing to the assembly of DNA–RNA–protein interactions at specific transcribed locations. Two lncRNAs, *Mistral* and *HOTTIP*, have been implicated in recruiting MLL, an H3K4 trimethylase to chromatin (34, 35).

1.5 LncRNAs in innate and adaptive immune signaling

The innate and adaptive immune responses provide immunity against a variety of pathogens. Innate immunity presents the first line of defense against pathogens. LncRNAs such as THRIL (36), lincRNA-Cox2, Lethe (37) and PACER (38) have been shown to regulate gene expression in innate immune cells. LincRNA-Cox2 regulates the expression of different sets of inflammatory genes in unstimulated and TLR2 ligand-stimulated macrophage cell line. The silencing of lincRNA-Cox2 up-regulates certain chemokines (CCL5, CX3CL1), chemokine receptors (CCR1), and interferon-stimulated genes (ISGs) (IRF7, OAS1A, OAS1L, OAS2, IFI204 and ISG15) in the unstimulated cells, but down-regulates TLR1, *IL6* and *IL23 in the stimulated cells*. This negative regulation of the genes is dependent on the interactions of lincRNA-Cox2 with heterogeneous nuclear ribonucleoprotein A/B and A2/B1 (39). Adaptive response is orchestrated through T and B lymphocytes. LncRNAs play a role in lineage-specific differentiation and activation of these cells. Several studies highlight the role of lncRNA in adaptive immune response including NRON (40), NeST (41), Gas5 (42, 43) and LncR-Ccr2-5’AS (44). Knockdown of lincRNA LincR-*Ccr2-5′*AS

results in impaired recruitment of T_H2 cells to the lungs (44). LincR-*Ccr2*-5′AS is expressed specifically on T_H2 subset of helper T cells and is regulated by GATA-3 transcription factor.

1.6 LncRNAs and influenza virus

The roles of lncRNAs in viral infections have been documented (45-50). Negative regulator of antiviral response (NRAV) is a lncRNA that is downregulated by various viruses including influenza virus, sendai virus, muscovy duck reovirus, and herpes simplex virus (48). Overexpression of NRAV increases virus replication whereas knockdown of NRAV has an opposite effect. The down-regulation of NRAV by influenza virus infection activates the marks of transcription (H3K4m3) and a decrease in repression signal of transcription (H3K27m3) at mxA and ifitm3 transcription start sites and thus regulates histone modification of these genes. Nuclear enriched abundant transcript 1 (NEAT1) upregulates interleukin-8 (IL8) transcription during influenza virus infection by recruiting splicing factor proline/glutamine-rich (SFPQ/PSF) to nuclear paraspeckle bodies (51). Gene regulation by lncRNA can also take place in a locus-specific manner. BST2 Interferon Stimulated Positive Regulator (BISPR) acts as a positive regulator of the flanking antiviral gene, bone marrow stromal cell antigen 2 (BST2) and dictates the potency of the antiviral interferon (IFN) response (52). Virus inducible lncRNA (VIN) is highly induced by influenza A virus and vesicular stomatitis virus, but not by interferons and is required for influenza virus replication (50). These studies suggest that lncRNAs play a crucial role in influenza virus pathogenesis.

Therefore, we perform studies to find out role of Wnt signaling and lncRNA in influenza virus infection with following objectives.

1.7 Objectives of the study

The objectives of these studies were to address the effect of Wnt signaling and iCRT14 on influenza virus replication and to find lncRNAs that are dysregulated during influenza virus infection. Furthermore, we wanted to see if these host factors are potential candidates for antiviral drug target.

CHAPTER II

MATERIALS AND METHODS

2.1 Cell Culture

A549 (human lung epithelial), human embryonic kidney (HEK) epithelial 293T and MDCK (Madin-Darby canine kidney epithelial) cells were purchased from ATCC (Manassas, VA). A549 cells were maintained in F12K medium with 10% fetal bovine serum (FBS) and 1% penicillin and streptomycin (PS). HEK, MDCK and Vero (African green monkey kidney epithelial) cells (ATCC) were maintained in DMEM with 10% FBS and 1% PS. E10 cells, a lung epithelial cell line, were kindly provided by Dr. M. Williams (Boston University) and were maintained in CMRL medium with 10% FBS, 1% PS and 2.5 mM L-Glutamax®.

2.2 Isolation of mouse primary epithelial cells.

Mouse alveolar epithelial cells type II (AEC II) were isolated from male C57BL/6 mice (8-10 weeks of age) as previously described (53). All the animal experiments were approved by the Institutional Animal Care and Use Committee (IACUC) at Oklahoma State University. Mice were anesthetized with ketamine and xylazine. The abdominal cavity was opened, and mice were exsanguinated by interrupting the abdominal aorta at the base of the heart and the lungs were cannulated with a 20-gauge catheter via the trachea. Lungs were perfused with solution II (10 mM HEPES, pH 7.4, 0.9% NaCl, 0.1% glucose, 5 mM KCL, 1. mM $MgSO_4$, 1.7 mM $CaCl_2$,

0.1 mg/ml streptomycin sulfate, 0.06 mg/ml penicillin G, 3 mM Na_2HPO_4 and 3 mM NaH_2PO_4), followed by instilling 1 ml of solution I (15 ml solution II plus 10 ml dispase from stock of 50 caseinolytic units/ml) through the trachea. Three lungs were isolated, pooled into a beaker containing ~10 ml of the solution I and incubated at 37°C for 45 min to release the AECs. After incubation, the lungs were chopped and further digested with the addition of DNase I (100 μg/ml) to solution I (10 ml) for 45 min at 37°C, with intermittent shaking. The digested lungs were filtered through 160-, 37- and 15-μm gauge nylon mesh sequentially. The filtrate was centrifuged at 250 *g* for 10 min. The cell pellet was resuspended in DMEM and incubated in a 100-mm-diameter Petri dish coated with mouse IgG (75 μg per dish) for 1 h. The cells were spun down at 250 *g* for 10 min and resuspended in DMEM containing 10% FBS. The yield was ~10×10^6 cells per 3 mice and the cell viability was >95%.

2.3 Preparation of Wnt3a Conditioned Medium

A stable cell line expressing soluble murine Wnt3a and a control murine L-cell line (ATCC) were maintained in DMEM supplemented with 10% FBS, 1% L-glutamine, and 0.4 mg/ml G418 (Invitrogen, Carlsbad, CA). To obtain Wnt3a_, or control (Con)_conditioned medium (CM), cells were cultured in fresh growth medium (DMEM with 10% FBS) without G418 for 4 days and then fresh G418-free medium for additional 3 days. The cultured media were mixed, sterile-filtered, and stored at −80°C until use. The activity of Wnt3a_CM was determined by a TOPflash assay performed in HEK 293T cells. Wnt3a_CM normally showed an approximately sevenfold increase in the reporter activity compared with Con_CM. 10X Wnt3a_CM or Con-CM were prepared by concentrating 20 ml CM into 2 ml using an ultrafiltration kit (Millipore, Billerica, MA).

2.4 Influenza virus stocks

Stocks of H1N1 strains of influenza virus A/PuertoRico/8/34 (A/PR/8/34), A/WSN/1933 (WSN) and A/Oklahoma/3052/09 (Pdm/OK) were propagated in the allantoic cavity of 10-day specific-pathogen-free embryonated chicken eggs (Charles River Laboratories, MA) at 35°C. The allantoic fluid was harvested, centrifuged at 2,000 g for 10 min, and stored at −80°C. Virus titer was determined by a Tissue Culture Infective Dose ($TCID_{50}$) assay. Briefly, MDCK cells were seeded in 96 well plates at a density of 25,000 cells per well. The next day cells were washed with serum-free medium twice. A series of ten-fold dilutions ranging from 10^{-1} to 10^{-8} were prepared in serum-free medium with 2 µg/ml L-1-Tosylamide-2-phenylethyl chloromethyl ketone treated trypsin (TPCK-trypsin). Cells were infected with each diluted virus stock in triplicate. After a 72 h culture, cells were analyzed for cytopathic effect (CPE) and $TCID_{50}$ was calculated using the Reed-Muench method (54).

2.5 Virus infection of the cells

Primary AEC II (0.25×10^6/well) were cultured in type I collagen-coated 12-well plates or cover slips for 6 days. All other cells were seeded at a density of 0.5×10^6 per well in 6-well plates for 24 h. The cells were washed with serum-free medium twice. The cells were infected with A/PR/8/34 or A/WSN/33 virus in serum-free medium containing TPCK-Trypsin (2 µg/ml) at a desired multiplicity of infection (MOI) at 37°C and 5% CO_2 incubator for 1 h. The cells were then washed with PBS once and complete medium was added. At 24 hrs post infection total viral mRNAs in cells and virus titers in media were determined.

2.6 Immunofluorescence

Alveolar epithelial cells were fixed with ice-cold 4% paraformaldehyde for 20 min and washed with PBS. The cells were permeabalized with 0.1% Triton X-100 for 10 min. Cells were

washed again and blocked with 5% goat serum. Cells were then incubated with hamster anti-T1α antibody (1:100 dilutions; E11, Developmental Studies Hybridoma Bank, University of Iowa) at 4˚C overnight, followed by incubation with Alexa fluor-488-conjugated anti-hamster secondary antibody (Life Technologies, Grand Island, NY) at 1:500 dilutions. Finally, cells were stained with 4' with 6-diamidino-2-phenylindole dihydrochloride (DAPI). Coverslips were mounted on glass slides for imaging.

2.7 Cell viability assay

iCRT14 (Tocris Bioscience, Minneapolis, MN) stock solution was prepared at 25 mM in dimethyl sulfoxide (DMSO) and then diluted to desired concentrations with respective media for different cell types. DMSO (0.05%) was used as a vehicle control. For cell viability assay A549 cells were seeded in 96 well plates at a density of 10^4/well. The next day, cells were treated with 12.5 µM iCRT14. The cells were collected at different times and cell viability was determined with CellTiter-Glo® Luminescent Cell Viability Assay (Promega, Madison, WI). This assay measures viable cells based on metabolic activity of the cells by quantifying cellular ATP content by luminescent signal.

2.8 RNA isolation and quantitative real-time PCR

Total RNAs were extracted using TRI Reagent (Molecular Research Center, Cincinnati, OH) and treated with DNase (Ambion, Grand Island, NY). For host mRNA, 1 µg of RNA was reverse-transcribed into cDNA using Oligo dT and random primers. Glyceraldehyde 3-phosphate dehydrogenase (GAPDH) was used as a housekeeping gene control. Different types of viral RNAs were quantified as described (55). One µg RNA was reverse-transcribed using strand- and sense-specific primers for vRNA (5'-AGCGAAAGCAGG-3' and 5'-AGCAAAAGCAGG-3'), cRNA (5'-AGTAGAAACAAGG-3'), and mRNA (Oligo dT). GAPDH specific primer (5'-GAAGATGGTGATGGGATTTC-3') was added to all reverse transcription reactions. Primers

used in this study are listed in Table 1. Real-time PCR was carried out with a 20 μl reaction mixture, which contained specific primers with SyBR green DNA dye (AnaSpec, Fremont, CA). The PCR conditions were performed on a 7900HT Fast Real-Time PCR System (Applied Biosystem, Foster City, CA) at cycling conditions of 95°C for 2 min, and 40 cycles of 95°C for 15 s and 60°C for 60 s. Data was normalized to as indicated in figures by ΔCT method.

Table 1. Real-time PCR primers

Gene Name	Forward primer	Reverse primer
PB1	GTCGAAAGGCTAAAGCATGGA	TGGCACTGAGATCTGCATGAC
PB2	CCGATGCCATAGAGGTGACA	GGAGACCAGCAGTCCAGCTTT
PA	GAAGTGCCATAGGCCAGGTTT	CAACGCCTCATCTCCATTCC
NA	TGTTGATGGAGCAAACGGAGTA	CTCAAACCCATGTCTGGAACTG
HA	GGCCCAACCACAACACAAAC	AGCCCTCCTTCTCCGTCAGC
IFNβ1	ATGACCAACAAGTGTCTCCTCC	GGAATCCAAGCAAGTTGTAGCTC
IFNα1	GCCTCGCCCTTTGCTTTACT	CTGTGGGTCTCAGGGAGATCA
GAPDH	GAAGGTGAAGGTCGGAGTC	GAAGATGGTGATGGGATTTC
AC015849.2	AACTGTCAAGCTCAATTTCCCTCT	GTGGAAAGGTTCGCTGGGAC
TAPSAR1	GGAAAGACATCGGACCGTCA	TGGGAAACGTTGGTGTCCTT
RP1-71H24.1	TTCCAGCTGTCTCCTAATTTCC	CTTTGTCCTGGTTGTCTTCCT
CTD-2639E6.9	AAGTCTGACTCCAGTCCCCG	GTTTGCGCTGCGAGATAAGG
PSORS1C3	CATCATGGCACACAACAACC	CCGGTCTAGGAAACCACTTATT
AC007283.5	GTACTTTGGGAGGCTGAGTG	CTGAAGTGCAGTGGTGTGA
RP11-670E13.5	AAATAGCATTTTGTACCCGCACT	GCCCGATTCCTCTTAGAAGGTT
OAS1	CCGGCGATTTAACTGATCCTG	TGTCCAAGGTGGTAAAGGGTG
OAS2	AGGTGGCTCCTATGGACGG	TTTATCGAGGATGTCACGTTGG
IL6	GGTACATCCTCGACGGCATCT	GTGCCTCTTTGCTGCTTTCAC
IP10	GTGGCATTCAAGGAGTACCTC	TGATGGCCTTCGATTCTGGATT
TLR7	TCCTTGGGGCTAGATGGTTTC	TCCACGATCACATGGTTCTTTG
ISG56	GCCATTTTCTTTGCTTCCCCTA	TGCCCTTTTGTAGCCTCCTTG
β-actin	GCCGGGACCTGACTGACTAC	TTCTCCTTAATGTCACGCACGAT
18S rRNA	CGTTGATTAAGTCCCTGCCCTT	TCAAGTTCGACCGTCTTCTCAG
UGGT2	CCTTCGCAATCTTGGGATCAA	GCCGGATCAATAAACAGAACCA
UBE2G2	ATCTACCCTGATGGGAGAGTCT	CTCCACTTTCGTCATTGGGC
GANAB	TGGGGATTACCCTTGCTGTG	CCGTATGCTTCTCTGTCGCT
BAG2	ATCAACGCTAAAGCCAACGAG	CGTCACTGATCTGCCTCATGT
SIL1	CTGCCTTCATCTAGGATGGCT	GGGTTGGTCAGGGCAAACTC
EIF2AK1	ACCCCGAATATGACGAATCTGA	CAAGTGCTCCAGCAAAGAAAC
UBE4B	CTACCTCCCCAATAGGTGCAT	GGCGAGCTGCTGAGAGAAC
TAP1	GGATTCTACAAGATGGCTCAG	TGTTGTTATAGATCCCGTCAC
snU2RNA	CATCGCTTCTCGGCCTTTTG	TGGAGGTACTGCAATACCAGG
PSMB8	CACGCTCGCCTTCAAGTTC	AGGCACTAATGTAGGACCCAG
M2	CGAGGTCGAAACGCCTATCAGAAAC	CCAATGATATTTGCTGCAATGACGAG
NS1	CCGACATGACTCTTGAGGAAAT	CGCCTGGTCCATTCTGATAC
NP	TGTGTATGGACCTGCCGTAGC	CCATCCACACCAGTTGACTCTTG

2.9 Animal Studies

Eight-week-old female C57BL/6J mice were infected with 1,000 pfu for a lethal challenge or 100 pfu for a sublethal challenge of influenza A virus (A/PR/8/34) in 50 µl volume via an intranasal route. Mice were treated by intraperitoneal injection of iCRT14 (50 mg/kg body weight) or DMSO as a vehicle control (4.2%) in a volume of 800 µl one day before virus infection and then daily from day 2 to day 5 as indicated. Mice were monitored for clinical symptoms such as arching back, huddling and ruffled fur. Body weight loss was monitored daily and mice which lost more than 30% body weight were euthanized and recorded as moribund and euthanized. For sublethal studies, clinical signs were scored as previously described (56): normal = 0, ruffled fur = 1, inactive = 3, hunched back and moribund = 4. Mice were sacrificed at day 2 and day 5 after infection. Left lungs were fixed in 10% neutral buffered formalin (Thermo Scientific, West Palm Beach, FL) and right lungs were snap-frozen in liquid nitrogen and used for RNA, protein and virus titer determination. For virus titer determination of lung tissues, right cranial lung lobes from infected mice were homogenized in 10% w/v phosphate-buffered saline (PBS) and were used for $TCID_{50}$ assay.

In a separate experiment, right lungs were used for collection of broncheoalveolar lavage (BAL) and left lungs were used for wet and dry ratio. Right lungs were lavaged with 500 µl ice cold PBS two time and approximately 80% volume was recovered. The BAL cells were spun down, resuspended and cytospin to slides. The slides were stained with dip quick stain (Jorvet, Loveland, CO). Differential cells counts were made with ≥ 400 cells per sample. The BAL fluid was frozen until use.

2.10 Lactate dehydrogenase (LDH) assay and total protein measurement

Lavage from the right lung lobe from each mouse of each group was used for LDH assay and total protein measurement. Fifty µls aliquots were used to measure the activity of LDH by monitoring the reduction of nicotinamide adenine dinucleotide at 340 nm in the presence of

lactate using a Thermo Scientific (Rockford, IL) LDH assay kit. Total protein in the BAL fluid was estimated by a modified Bradford assay according to the manufacturer's instructions (Biorad), and the remainder was frozen at −80 °C until processed.

2.11 Histopathologic analyses

Animals were euthanized by exsanguinations of abdominal aorta under Xylazine and Ketamine anesthesia as per approved IACUC protocol. Formaline-perfused lungs were embedded in paraffin wax. Sections of 4 µm thickness were cut and stained with hematoxylin and eosin (H&E). Histopathologic lesions were scored by a board certified pathologist as described (57): 1 = minimal damage to alveolar structures, 2 = mild, 3 = moderate and 4 = marked/severe damage to lung tissue.

2.12 RNA sequencing and data analysis

A549 cells were infected with PR/8 at a MOI of 2 for 24 h. Total RNAs from 3 control and 3 infected cells were extracted. RNA-seq was performed by Applied Biological Materials, Inc. **(**Richmond, BC, Canada). RNA quality check was performed using the Agilent 2100 Bioanalyzer. All samples were subjected to polyA enrichment, followed by first and second strand synthesis, adenylation of 3' ends, adapter ligation, DNA fragment enrichment, and real-time PCR quantification. Up to twenty-five million paired-end reads for each sample were generated. Paired-end reads were directionally mapped to the genomic loci of lncRNA (GRCh37 /hg19) by TopHat2. CuffDiff analysis was then run to identify the dysregulated lncRNAs. Gene ontology (GO) functional annotation of mRNA expression profile was conducted by STIRNG analysis (http://string-db.org/). KEGG pathway enrichment in the altered mRNAs was also performed by STIRNG analysis. STRING is a web-based tool to investigate protein-protein interactions, KEGG pathway, and GO annotation.

2.13 Interferon treatment and lncRNA induction

A549 cells were seeded in 12-well plates and cultured overnight. Cells were then treated with 1,000 U/ml human IFNβ1a (#11415-1, PBL assay science, Piscataway Township, NJ) in F12-K medium with 10% FBS and 1% PS for different times as indicated. At each time point, RNA was extracted for real-time PCR analysis.

2.14 Lentiviral shRNA vector construction

Lentiviral shRNA were constructed as previously describes (58). LncRNA-specific shRNA oligos (Table 2) were designed using BLOCK-iT™ shRNA Designer by Thermo Fischer Scientific (Grand Island, NY). The lentiviral vector that contained an irrelevant sequence was used as a negative control. For each lncRNA 3 different oligos were designed and shRNA vectors were prepared. Briefly, the oligos were annealed and ligated into the pSIH-H-copGFP vector (System Biosciences, Mountain View, CA) digested with *BamH* and *EcoR1* restriction enzymes. These plasmids were transformed into STBL 3 cells and two colonies for each pair of oligos were selected from LB agar after overnight incubation. Colonies were propagated in LB broth overnight, plasmids were isolated and sequenced. Sequence confirmed designs were used for preparing lentivirus to knockdown lncRNAs.

Table 2. Oligos used for constructing lncRNA shRNAs

LncRNA name	shRNA Primers
AC015849.2-FW1	GATCCGGACGAGTAGGAAAGTCATTCTTCAAGAGAGAATGACTTTCCTACTCGTCCTTTTTG
AC015849.2-RE1	AATTCAAAAAGGACGAGTAGGAAAGTCATTCTCTCTTGAAGAATGACTTTCCTACTCGTCCG
AC015849.2-FW3	GATCCGGTGAACTGTCAAGCTCAATTTTCAAGAGAAATTGAGCTTGACAGTTCACCTTTTTG
AC015849.2-RE3	AATTCAAAAAGGTGAACTGTCAAGCTCAATTTCTCTTGAAAATTGAGCTTGACAGTTCACCG
TAPSAR1-FW1	GATCCGGACACCAACGTTTCCCATTCTTCAAGAGAGAATGGGAAACGTTGGTGTCCTTTTTG
TAPSAR1-RE1	AATTCAAAAAGGACACCAACGTTTCCCATTCTCTCTTGAAGAATGGGAAACGTTGGTGTCCG
TAPSAR1-FW2	GATCCGCTCAGAAGGATTCCTAATGATTCAAGAGATCATTAGGAATCCTTCTGAGCTTTTTG
TAPSAR1-RE2	AATTCAAAAAGCTCAGAAGGATTCCTAATGATCTCTTGAATCATTAGGAATCCTTCTGAGCG
RPI-71H24.1-FW1	GATCCGCTTCCAGCTGTCTCCTAATTTTCAAGAGAAATTAGGAGACAGCTGGAAGCTTTTTG
RPI-71H24.1- RE1	AATTCAAAAAGCTTCCAGCTGTCTCCTAATTTCTCTTGAAAATTAGGAGACAGCTGGAAGCG
RPI-71H24.1- FW2	GATCCGGAAGACAACCAGGACAAAGATTCAAGAGATCTTTGTCCTGGTTGTCTTCCTTTTTG
RPI-71H24.1- RE2	AATTCAAAAAGGAAGACAACCAGGACAAAGATCTCTTGAATCTTTGTCCTGGTTGTCTTCCG
RPI-71H24.1- FW3	GATCCGGCAAGACTGCAACAGTATTGTTCAAGAGACAATACTGTTGCAGTCTTGCCTTTTTG
RPI-71H24.1- RE3	AATTCAAAAAGGCAAGACTGCAACAGTATTGTCTCTTGAACAATACTGTTGCAGTCTTGCCG
CTD-2639E6.9- FW1	GATCCGGATCCGGAGACTCCTTATCTTTCAAGAGAAGATAAGGAGTCTCCGGATCCTTTTTG
CTD-2639E6.9- RE1	AATTCAAAAAGGATCCGGAGACTCCTTATCTTCTCTTGAAAGATAAGGAGTCTCCGGATCCG
CTD-2639E6.9- FW2	GATCCGCAACACTCCATCTTCCAGAGTTCAAGAGACTCTGGAAGATGGAGTGTTGCTTTTTG
CTD-2639E6.9- RE2	AATTCAAAAAGCAACACTCCATCTTCCAGAGTCTCTTGAACTCTGGAAGATGGAGTGTTGCG
CTD-2639E6.9- FW3	GATCCGCAAACCTCAGGCAACTACAGTTCAAGAGACTGTAGTTGCCTGAGGTTTGCTTTTTG
CTD-2639E6.9- RE3	AATTCAAAAAGCAAACCTCAGGCAACTACAGTCTCTTGAACTGTAGTTGCCTGAGGTTTGCG
PSORS1C3- FW1	GATCCGGTCGAGAGCAAGTCTCTATTTTCAAGAGAAATAGAGACTTGCTCTCGACCTTTTTG
PSORS1C3- RE1	AATTCAAAAAGGTCGAGAGCAAGTCTCTATTTCTCTTGAAAATAGAGACTTGCTCTCGACCG
PSORS1C3- FW2	GATCCGAGCATCATGGCACACAACAATTCAAGAGATTGTTGTGTGCCATGATGCTCTTTTTG
PSORS1C3- RE2	AATTCAAAAAGAGCATCATGGCACACAACAATCTCTTGAATTGTTGTGTGCCATGATGCTCG
PSORS1C3- FW3	GATCCGTCGAGAGCAAGTCTCTATTGTTCAAGAGACAATAGAGACTTGCTCTCGACTTTTTG
PSORS1C3-RE3	AATTCAAAAAGTCGAGAGCAAGTCTCTATTGTCTCTTGAACAATAGAGACTTGCTCTCGACG
RP11-670E13.5- FW1	GATCCGCCCACAACACAATCACTCTCTTCAAGAGAGAGAGTGATTGTGTTGTGGGCTTTTTG
RP11-670E13.5- RE1	AATTCAAAAAGCCCACAACACAATCACTCTCTCTCTTGAAGAGAGTGATTGTGTTGTGGGCG
RP11-670E13.5- FW2	GATCCGCCTCAGTAAAGTCCACCCTGTTCAAGAGACAGGGTGGACTTTACTGAGGCTTTTTG
RP11-670E13.5- RE2	AATTCAAAAAGCCTCAGTAAAGTCCACCCTGTCTCTTGAACAGGGTGGACTTTACTGAGGCG

2.15 Lentivirus preparation and infection

Lentivirus particles were produced in HEK293T cells using Lenti-X HTX Packaging Mix (Clontech, Mountain View, CA). HEK293T cells in 10-cm dishes at 50%–70% confluency were

transfected with 3 μg of packing plasmids and 3 μg of lentiviral shRNA plasmid using Lipofectamine 2000 (Life Technologies). Fresh DMEM media containing 10% FBS was added 24 h after transfection. The cell culture supernatant was collected after a 48 h culture and centrifuged at 100 g for 10 min. The supernatant containing the lentivirus was aliquoted and stored at -80 ºC for future use. The viral titers were determined by infected HEK293T cells with a series of 10-fold dilutions of viral stock in the presence of 4 μg/ml of polybrene. The medium was changed after 24 h infection and GFP-positive cells were counted after additional 48 h culture. Virus titer was calculated determined based on this formula, infectious particle/ml = (Average of GFP positive cells from 10 random fields*594)/ (dilution factor*volume of infection) where 594 is fields/well (20X objective) in a 12 well plate.

For knockdown experiments, A549 cells were infected with a shRNA lentivirus in the presence of 4 μg/ml of polybrene at a MOI of 100 for 48 h. The infection efficiency was monitored by green fluorescent protein under a fluorescent microscopy. The knockdown efficiency of lncRNAs was determined by real-time PCR.

2.16 Western blot analysis

Cells were lysed in M-PER™ Mammalian Protein Extraction Reagent (Thermo Fischer, Waltham, MA). Proteins (30 μg/lane) were separated by 12% of SDS-PAGE and transferred onto nitrocellulose membranes using Trans-Blot® Turbo™ Transfer System (Bio-Rad, Hercules, CA). Membranes were blocked with 5% non-fat milk and then probed with different primary antibodies prepared in 5% non-fat milk overnight. Membranes were washed with TRIS-buffered saline for 5 min × 3 times and incubated with species-appropriate horseradish peroxidase-labeled secondary antibody for 1 h at room temperature. Membranes were again washed with TRIS-buffered saline for 5 min × 3 times. Finally, the membranes were developed using SuperSignal™ West Pico Chemiluminescent Substrate (Thermo Fischer, Waltham, MA). Protein bands were detected with Amersham Western blot detection system (GE healthcare system, Pittsburgh, PA).

Protein levels were normalized to glyceraldehyde-3-phosphate dehydrogenase (GAPDH) and quantitation was determined using Image Quant software from GE healthcare system. The primary antibody against GAPDH (cat# G8795) was purchased from Sigma-Aldrich (St. Louis, MO). Influenza viral protein antibodies, NP (cat# MCA400), NS1 (cat# SC-130568), and M2 (cat# MA1-082) were purchased from AbD serotech (Raleigh, NC), Santa-Cruz biotechnology (Paso Robles, CA) and Thermo Fischer (Waltham, MA), respectively. Antibody dilutions were 1:2,000 for GAPDH, 1:500 for NP, 1:1,000 for NS1, and 1:5,000 for M2. HRP-conjugated secondary antibodies against mouse (cat#115-0.5-003) and rabbit (cat#111-035-003) were purchase from Jackson Immuno Research (West Grove, PA) and used at a dilution of 1: 2,000 and 1: 10,000 respectively.

2.17 Isolation of cytoplasmic and nuclear RNAs

Cytoplasmic and nuclear fractions were prepared from A549 cells using a kit (#21000, Norgen, Canada). cDNA was prepared using 1 µg RNA and real-time PCR was performed to analyze both cellular fractions using primers for β-actin, GAPDH, TAPSAR1 and U2snRNA. The expression of mRNA or lncRNA in nucleus and cytoplasm was calculated with the equation 2^{-Ct}. The percentage of each RNA in the nucleus and cytoplasm were calculated.

2.18 Data analysis

Data from at least three independent experiments was analyzed. The results were statistically analyzed using Student's t-test or One-way ANOVA, followed by Tukey's post hoc analysis. *P* values of <0.05 were considered significant.

CHAPTER III

RESULTS

3.1 Activation of Wnt/β-catenin signaling increases influenza virus replication

To examine whether Wnt/β-catenin signaling affects influenza virus replication, we determined the effects of activation of the Wnt/β-catenin signaling using Wnt3a_CM on influenza viral gene expression. Mouse lung epithelial cells, E10 were pretreated with Wnt3a_CM and then infected with A/PR/8/34 for 18 h. Wnt3a_CM increased mRNA expression of the viral genes hemagglutinin (HA), M1 matrix protein (MP) and nucleoprotein (NP) (Fig. 3.1A). When mice were pre-treated with Wnt3a_CM and then infected with A/PR/8/34, increases in mRNA levels of HA, MP and NP in the lungs were also observed (Fig. 3.1B). These results indicate that Wnt3a treatment activation increased influenza virus replication.

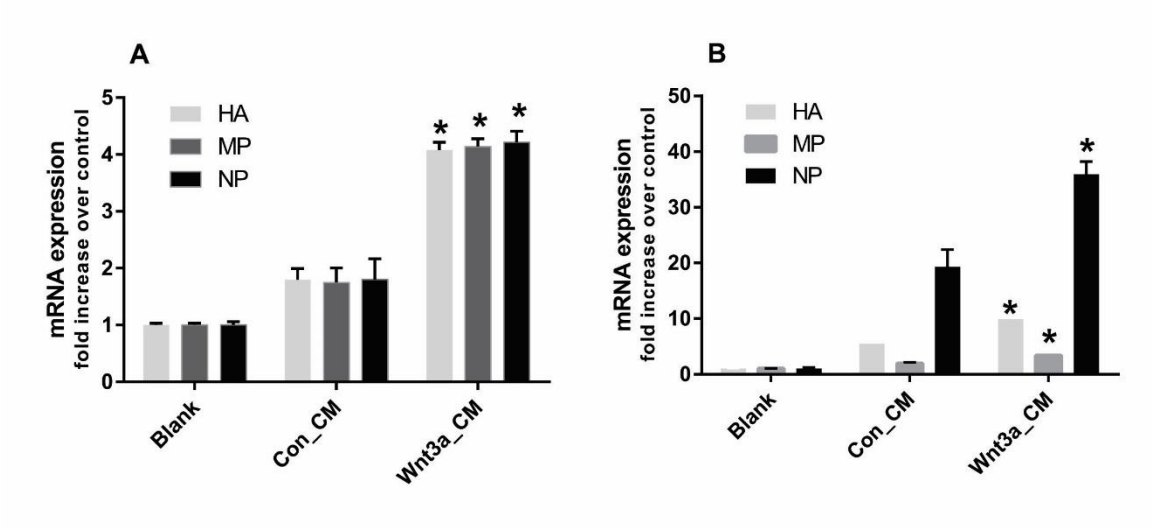

Figure 3.1 Wnt3a increases influenza viral gene expression. (A) E10 cells were pretreated with 50% Wnt3a_CM or Con_CM for 24 h and infected with influenza virus A/PR/8/34 at a MOI of 1 for 18 h. (B) Mice were instilled with 10x Wnt3a_CM or Con_CM followed by PR/8 infection (250 pfu/mice) and the lungs were collected on day 5 post infection. Relative mRNA expression levels of viral genes (HA, NP and MP) were measured by real-time PCR and normalized to GAPDH. Data is normalized to blank control and represented as mean ± SE (n = 4). $p < 0.05$ vs. Con_CM (Students t-test).

3.2 iCRT14 inhibits influenza virus infection.

We next examined the effect of inhibiting Wnt/β-catenin signaling on influenza virus infection. iCRT14 is a small molecule that inhibits Wnt/β-catenin signaling by preventing the binding of β-catenin with LEF/TCF transcription factor (16, 27) and was used for this study. Human alveolar epithelial cells (A549) were treated with 12.5 μM iCRT14 for 12 h and then infected with A/PR/8/34 at a MOI of 1 for different times. Infectious virus particles released into the medium were quantified using a $TCID_{50}$ assay. Virus titers in the iCRT14-treated cells were significantly reduced at 12 and 48 h post infection (hpi) compared to the control cells (Fig. 3.2A).

Similar results were observed with A/WSN/33 virus (Fig. 3.2B). This effect was not due to the toxicity of iCRT14 because iCRT14 had no effects on cell viability (Fig. 3.2C). These results indicate that iCRT14 has antiviral activity against different strains of influenza A virus.

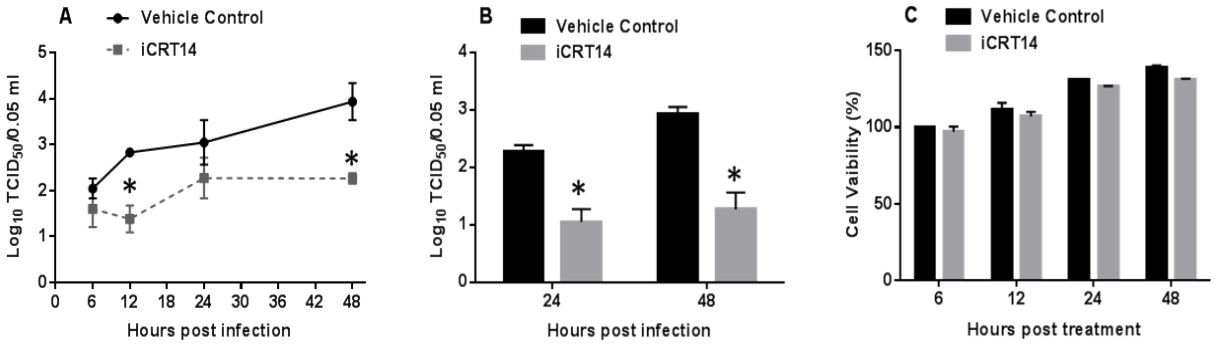

Figure 3.2. iCRT14 reduces influenza virus infection. (A, B) A549 cells were treated with iCRT14 (12.5 μM) or vehicle control for 12 h and then infected with A/PR/8/34 (A) or A/WSN/33 (B) at a MOI of 1. Media were collected at different times post infection and titers were determined by $TCID_{50}$ assay. (C) A549 cells were treated with iCRT14 (12.5 μM) or vehicle control for various times and cell viability was measured by CellTiter Glo kit (Promega). Results of 3 independent experiments are displayed as mean ± SE. *P<0.05 vs. vehicle control at the corresponding time points (Student's t-test).

3.3 iCRT14 acts on the early stage of the influenza virus life cycle

Influenza virus undergoes several steps of its life cycle in the host cell from entry to budding (59). To determine which stage of the viral life cycle was inhibited by iCRT14, we added the inhibitor at different times before and after infection and determined virus titers in the media at 12 hpi. When it was added 1 h before and up to 5 hpi, iCRT14 decreased virus titers (Fig. 3.3). However, iCRT14 had no effects on virus titers when it was added at 7 and 9 hpi. The result indicates that iCRT14 acts at the earlier stages at or before virus gene transcription.

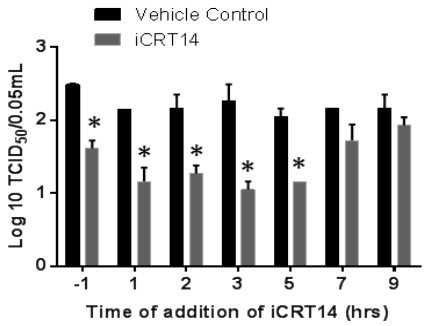

Figure 3.3 Effect of iCRT14 on stages of the influenza virus life cycle. A549 cells were infected with A/PR/8/34 at a MOI of 1. Cells were treated with iCRT14 (12.5 μM) or vehicle control at different times before or after infection. Media were collected 12 h post infection and titers were determined by $TCID_{50}$ assay. Results of 3 independent experiments are displayed as mean ± SE. *P<0.05 vs. vehicle control at the corresponding time points (Student's t-test).

3.4 iCRT14 reduces influenza virus RNA synthesis

The influenza virions contain negative sense RNA (vRNA). The RNA synthesis of influenza virus occurs in three steps: (i) vRNA is transcribed into mRNA by cap snatching mechanism via RNA-dependent RNA polymerase enzyme, (ii) intermediate cRNA is synthesized from vRNA, and (iii) cRNA is copied to full length negative sense vRNA for new progeny virus particles (55, 60). We further examined the effect of iCRT14 on the expression level of different types of influenza viral RNAs. A549 cells were treated with iCRT14 (12.5 μM) 1 h before infection and infected with A/PR/8/34 at a MOI of 5 for 5 h and cRNA, vRNA, and mRNA were measured with Real-time PCR. Ribavirin inhibits influenza virus RNA synthesis by inhibiting the polymerase complex (61) and was used as a positive control for this experiment. Similar to ribavirin, iCRT14 markedly reduced the levels of vRNA, cRNA and mRNA of all 8 segments including polymerase basic 1 (PB1), polymerase basic 2 (PB2), polymerase acidic (PA), HA, nucleoprotein (NP), NA, MP and non-structural protein (NS) (Fig. 3.4A, B, C). This effect was dose-dependent (Fig 3.4D, E). The results showed that iCRT14 inhibits viral gene replication and transcription.

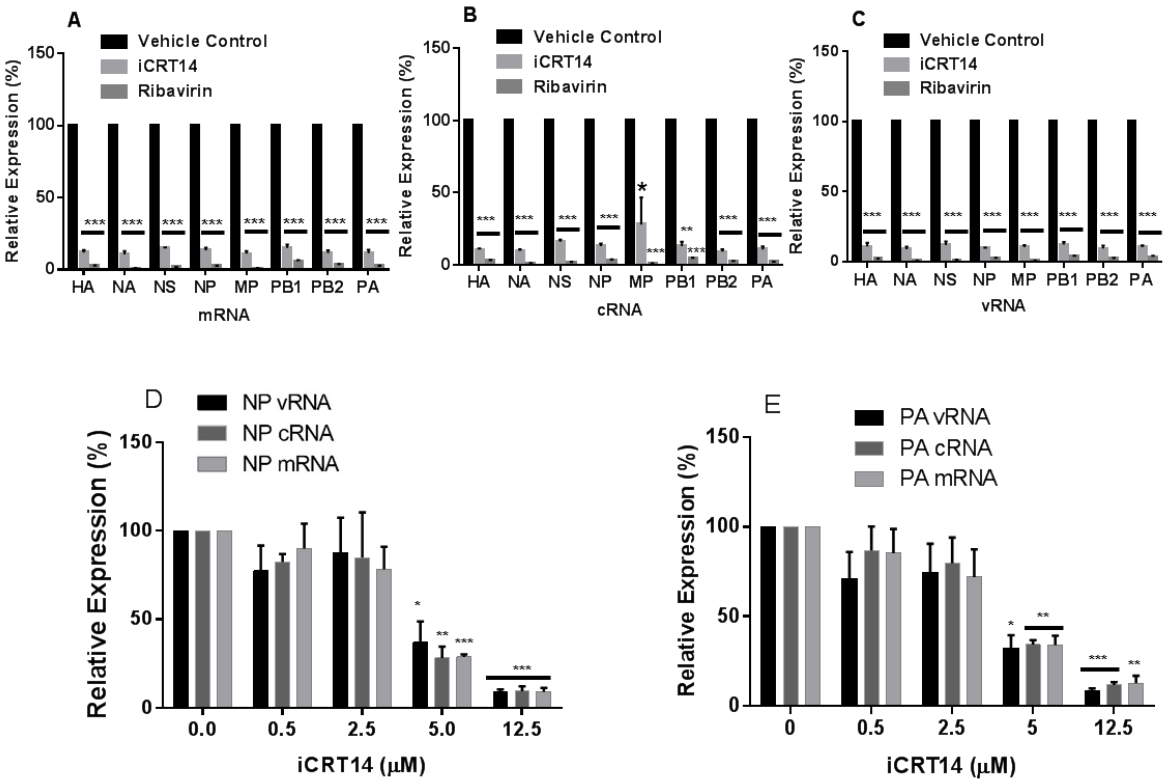

Figure 3.4 iCRT14 effect on influenza virus RNA synthesis. A549 cells were infected with A/PR/8/34 at a MOI of 5. Cells were treated with iCRT14 at 12.5 μM (A, B, C) or at indicated concentrations (D, E) at 1 h before infection. RNA was extracted at 5 h post infection. mRNA, cRNA, and vRNA levels of viral genes were determined by real-time PCR and normalized to GAPDH. Data was expressed as a percentage of vehicle control. Results of 3 independent experiments were displayed as mean ± SE. *P<0.05 vs. vehicle control, **P<0.01 vs. vehicle control, ***P<0.001 vs. vehicle control (Student's t-test).

3.5 Antiviral activity of iCRT14 is independent of interferon production

Interferons (IFNs) are the first line of defense against influenza virus. Influenza virus infection induces IFN production that is required for mounting a proper antiviral response (62). We designed two sets of experiments to test whether IFNs are involved in the antiviral activity of iCRT14. First, we examined the effects of iCRT14 on A/PR/8/34-induced IFN gene expression. A/PR/8/34 induced the mRNA expression of IFNα1 and IFNβ1 in A549 cells. However, iCRT14 had no effect on this induction (Fig. 3.5A, B). Second, we repeated the experiment described in fig. 3.4 using Vero cells, which are deficient in IFN production (63, 64). Nevertheless, iCRT14 reduced the levels of vRNA, cRNA and mRNA of the NP gene in Vero cells as it did in A549 cells (Fig. 3.5C). These results suggest that the antiviral activity of iCRT14 is independent of the IFN response.

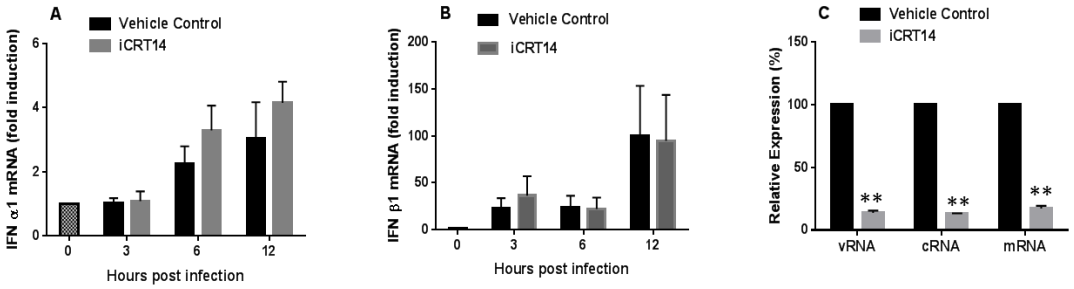

Figure 3.5 iCRT14-mediated inhibition of influenza virus RNA synthesis is independent of the IFN response. (A, B) A549 cells were infected with A/PR/8/34 at a MOI of 1 for different times. Cells were treated with iCRT14 (12.5 μM) or vehicle control 1 h before infection. IFN α1 and β1 mRNA levels were determined by real-time PCR and normalized to GAPDH. Data was expressed as fold change over mock infection. (C) Vero cells were infected with A/PR/8/34 at a MOI of 5. Cells were treated with iCRT14 (12.5 μM) or vehicle control 1 h before infection. cRNA, vRNA and mRNA levels of NP gene were determined at 5 h post infection using real-time PCR and normalized to GAPDH. Data is expressed as a percentage of vehicle control. Results of independent experiments are presented as means ± SE. *P<0.05 vs. vehicle control (Student's t-test)

3.6 iCRT14 reduces influenza virus infection in primary alveolar epithelial cells

AECs are one of the primary targets of influenza virus. We examined if iCRT14 also reduces influenza virus infection in primary AECs. AEC II were isolated from mice and cultured for 6 days to allow them to differentiate into AEC I (53, 65, 66). The day 6 cells showed a uniform staining of the AEC type I marker T1α (Fig. 3.6A). We treated these cells with iCRT14 or vehicle and infected with A/PR/8/34 or A/WSN/33 at a MOI of 1 for 24 h and measured virus titers in the media and NA mRNA in the cells. We found that iCRT14 reduced virus titers (Fig. 3.6B, C) and NA mRNA levels (Fig. 3.6D, E) in both A/PR/8/34 and A/WSN/33 infected cells. Our results indicate that iCRT14 is also effective in repressing influenza virus infection in primary AECs.

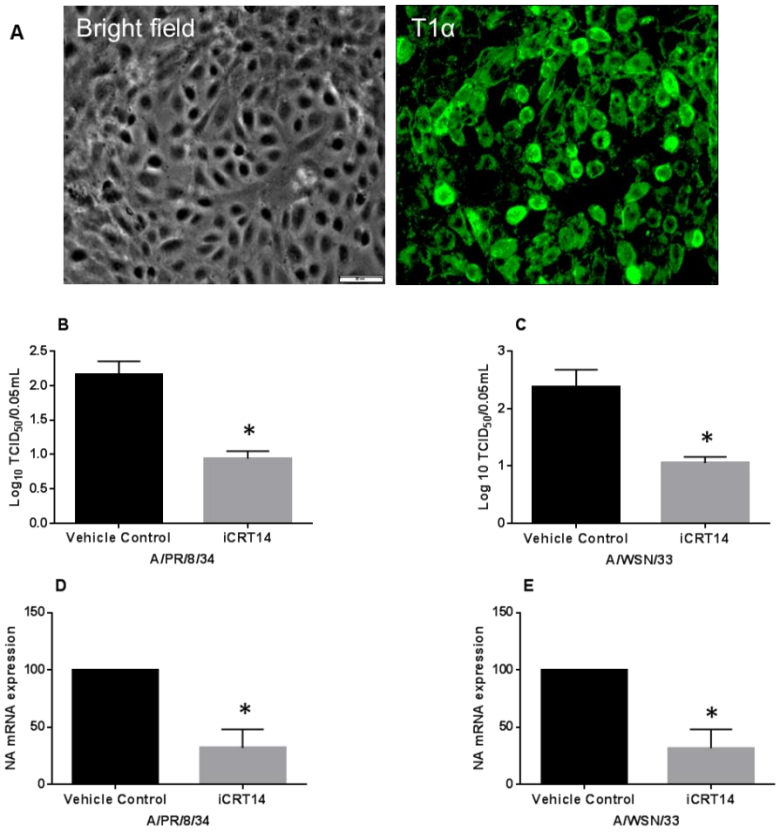

Figure 3.6. Effect of iCRT14 on influenza virus infection in primary mouse alveolar epithelial cells (AECs). Mouse AECs were isolated from mice and cultured for 6 days. (A) AECs were immuno-stained with AEC type I maker, T1α and nuclear dye, DAPI. Scale bar = 50 μm. (B-E) AECs were infected with A/PR/8/34 or A/WSN/33 at a MOI of 1 for 24 h. Cells were treated with iCRT14 (12.5 μM) or vehicle control 1 h before infection. Titers in media were determined using $TCID_{50}$ assay (B, C). NP mRNA levels in cells were determined by real-time PCR and normalized to GAPDH. Results of 3 independent experiments are displayed as mean ± SE. *$P<0.05$ vs. vehicle control at the corresponding time points (Student's t-test).

3.7 iCRT14 partially protects mice from a lethal dose of influenza virus challenge

To test whether iCRT14 protected mice from influenza virus infection, we performed a survival study with a lethal dose of influenza virus A/PR/8/34 (1,000 pfu/mouse). Mice were treated with iCRT14 (50 mg/kg body weight) one day before infection and daily thereafter until day 6 after infection. The dose was chosen based on reports from other groups for tumor studies (16, 67). The results showed that iCRT14-treated mice exhibited a slightly less body weight loss at day 8 (Fig. 3.7A) and a slight improvement in survival time (Fig. 3.7B).

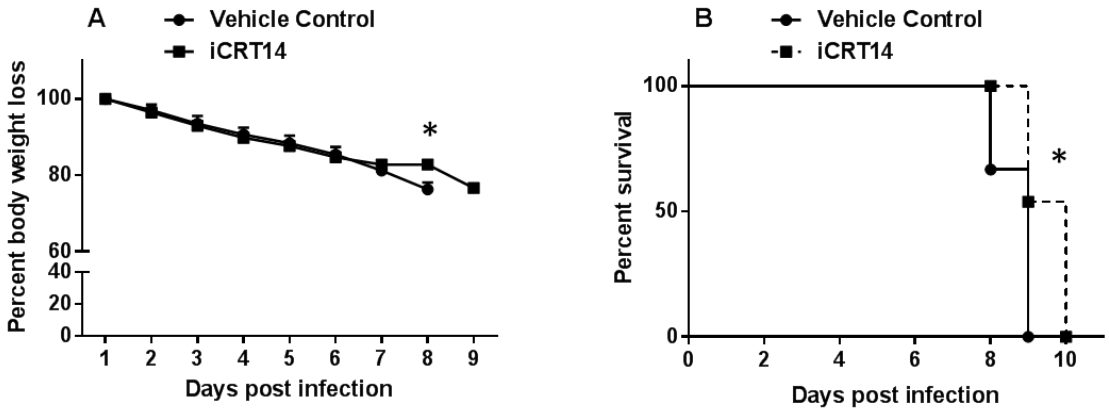

Figure 3.7 Effects of iCRT14 on weight loss and survival rate in mice challenged with a lethal dose of A/PR/8/34. C57BL/6J mice were treated with iCRT14 (50 mg/kg) or vehicle control one day before infection daily until day 6 post infection. The mice were challenged with A/PR/8/34 (1,000 pfu/mouse). (A) Percent of body weight loss. Body weight loss is presented as mean ± SE. *$p < 0.05$ vs. vehicle control at day 8 (Student t-test). (B) Kaplan–Meier survival curves of iCRT14 and vehicle control groups. Mantel-Cox χ^2 test was used for analysis *$P< 0.05$, n = 12 – 13 animals per group

3.8 iCRT14 attenuates clinical signs associated with a sublethal dose of influenza virus challenge

In our survival study, 30% body weight loss necessitated euthanasia. However, human patients with flu infection normally do not lose that much body weight (8). Thirty percent weight loss in mice corresponds to human patients with severe acute respiratory distress syndrome caused by influenza virus (68, 69) and therefore survival study in mice does not necessarily mimic human disease conditions. We thus performed a sublethal dose of A/PR/8/34 challenge (100 pfu/mouse) in mice and examined virus loads and lung pathology. Under these conditions, no mortality was observed in both control and iCRT14-treated groups. iCRT14 significantly reduced virus titers in the lung tissues at 2 and 5 days post infection (Fig. 3.8A). There was no difference in clinical scores at day 2 post infection between iCRT14-treated and control mice. However, at 5 days after infection, iCRT14-treated mice showed significant lower clinical scores compared to control mice (Fig. 3.8B). The mice treated with iCRT14 had a decreased wet-to-dry ratio, an indicator of extravascular edema in lungs, at 5 days after infection (Fig. 3.8C). However, we did not observe differences in total protein, number of inflammatory cells (macrophages, neutrophils and lymphocytes) and LDH activity in BAL between iCRT14-treated and control groups (Fig. 3.8D, E, F), suggesting that iCRT14 does not improve alveolar leakage, cell injury and inflammation.

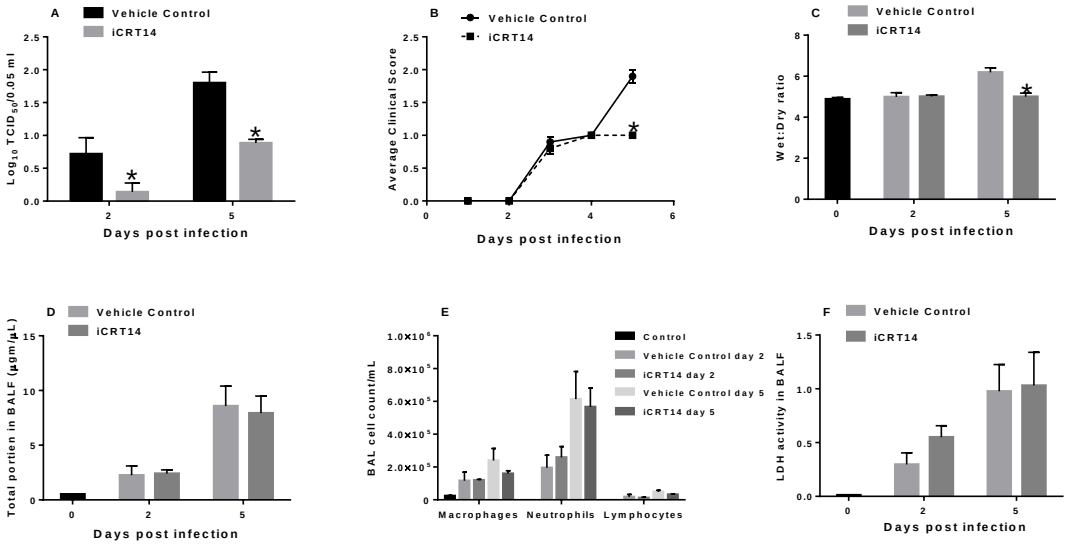

Figure 3.8 Effect of iCRT14 on lung injury and inflammation of mice with a sub-lethal dose of A/PR/8/34 challenge. C57BL/6J mice were infected with A/PR/8/34 (100 pfu/mouse). Mice sacrificed on the day 0 of study were used as a control. Mice received either iCRT14 (50 mg/kg) or vehicle control daily beginning one day before infection until day 2 or day 5 after infection. (A) Virus titers in total lung homogenate (n=6). (B) Average clinical scores. 0 = Normal, 1 = Ruffled fur, 2 = Inactive, 3 = Hunched back (n = 10 – 20). (C) Lung water content as measured by wet-to-dry ratio. n = 4. (D) Total proteins in BAL fluid. n = 4. (E) LDH activity in BAL fluid n = 4. (F) Inflammatory cells in BAL. n = 3 – 4. All the data are presented as mean ± SE. *P < 0.05 vs. vehicle control at the corresponding days.

3.9 Effect of iCRT14 on lung histopathology of mice with a sub-lethal dose of A/PR/8/34 challenge.

H & E staining revealed that at day 2 post infection iCRT14 equivocally reduced epithelial degeneration and/or necrosis in major airways when compared to vehicle control (Table 3). At day 5 post infection there was decrease attenuation of epithelium and loss of cilia with the treatment of iCRT14. There was subtle decrease in severity of the lung lesions such as alveolar histiocytic infiltration and neutrophilic and histiocytic infiltration in major airways in the treatment group at day 5 post infection when compared to control group. (Figure 3.9, Table 3).

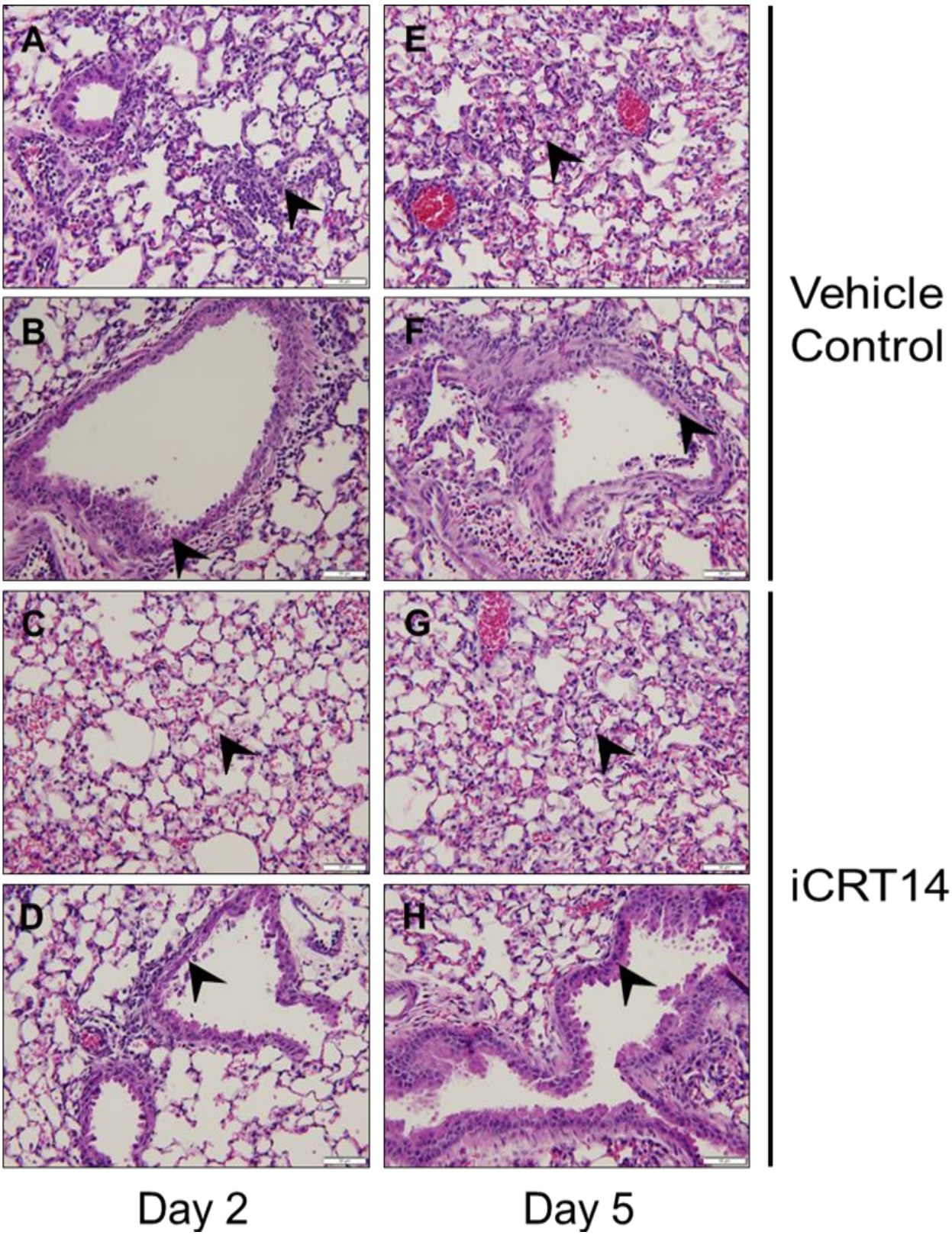
A
E
B
F
C
G
D
H
Vehicle Control
iCRT14
Day 2
Day 5

Figure 3.9 histopathology of mice lungs with a sub-lethal dose of A/PR/8/34 challenge and treated with iCRT14. C57BL/6J mice were infected with A/PR/8/34 (100 pfu/mouse). Mice received either iCRT14 (50 mg/kg) or vehicle control daily beginning one day before infection until day 2 or day 5 after infection. Representative H&E photomicrographs from 6 mice are shown. A, B = day 2 vehicle control mice; C, D = day 2 iCRT14 mice; E, F = day 5 vehicle mice; G, H = day 5 iCRT14 mice. Dark arrowheads represent alveolar histiocytic and neutrophil infiltrations with associated hemorrhage in Panels A, C, E, G. Arrowheads represent major airway degeneration/necrosis, histiocytic and neutrophil infiltration in Panels B, D, F, H. Scale bar = 50 μm.

Table 3: Histopathology of the lungs of mice infected with a sublethal dose of influenza virus on day 2 and 5 post-infection.

Microscopic Findings in Lung	**Treatment Groups**											
	Vehicle control						**iCRT14 (50 mg/kg)**					
Animal #	7	8	9	10	11	12	13	14	15	16	17	18
2 days post infection												
Major airways: Epithelial degeneration and/or necrosis	3M	--	3M	3M	--	2M	2M	2M	2M	2M	3M	2M
5 days post infection												
Animal #	19	20	21	22	23	24	25	26	27	28	29	30
Alveolus: Histiocyte infiltration	3M	3M	3M	3M	3M	2M	3M	2M	2M	1M	3M	3M
Major airways: Attenuated epithelium with loss of cilia	3M	2M	3M	3M	3M	2M	2M	1M	1M	2M	2M	2M
Major airways: Neutrophil and histiocyte infiltration	3M	2M	3M	3M	2M	2M	3M	2M	1M	1M	2M	3M
Severity: -- = not present; 1 = minimal; 2 = mild; 3 = moderate Distribution: F = focal; M = multifocal												

3.10 iCRT14 toxicity

Finally, we evaluated whether iCRT14 causes toxicity in mice. Mice were treated with iCRT14 at doses of 50 and 100 mg/kg or vehicle control every day for 9 days via intraperitoneal route. Major organs including liver, lung, heart, kidney, stomach, small intestine, eyes and brain were processed for histopathological analysis. Microscopic lesions were scored by a pathologist. Major organ toxicity was not identified with iCRT14 treatment at either doses of iCRT14.

3.11 LncRNAs are differentially expressed in influenza virus-infected A549 cells

To identify lncRNAs that are dysregulated during influenza virus infection, we infected lung epithelial A549 cells with PR/8 at a MOI of 2 for 24 h and performed RNA-seq analysis. Tophat was used for read mapping and Cufflinks/Cuffdiff was used for gene expression quantification. Figure 3.10A depicts the design of the experiment. Using a p value of < 0.05, we found that 8,983 mRNAs were significantly changed by PR/8 infection (Fig. 3.10B). Of them, 3,649 mRNAs were upregulated and 5,334 mRNAs were downregulated (Fig. 3.10C). 1,625 up-regulated and 2,784 down-regulated mRNAs were changed 2-fold or more (Table 4). The numbers of mRNAs with various fold changes are also listed in Table 4. Up-regulation of ISGs was observed (Table 5), indicative of successful influenza virus infection.

Similarly, we identified 1,912 lncRNAs that were significantly changed in PR/8-infected A549 cells (Fig. 3.10D). Of them, 716 lncRNAs were up-regulated and 1,196 lncRNAs were down-regulated (Fig. 3.10E). There were 418 up-regulated and 683 down-regulated lncRNAs based on a fold change of 2 or more. Interestingly there were only 11 down-regulated lncRNAs compared to 68 up-regulated lncRNAs based on a fold change of > 100 (Table 4).

Given a greater number of lncRNAs that are up-regulated compared to the down-regulated lncRNAs during influenza virus infection based on a fold change of > 100 (Table 4), we decided to focus on the up-regulated lncRNAs for further studies. To narrow down our

selection, we used the following criteria: (a) a fold change of >2 for up-regulated lncRNAs, (b) significant changes in the expression of neighboring genes (up or down) within 10,000 kb of lncRNAs, (c) neighboring genes involved in > 5 pathways based on GO analysis, and (d) >500 base pair long with no ORF (open reading frame). Seven lncRNAs met these criteria and are listed in Table 6 and marked in yellow color in the scatter plot (Fig. 3.10B). These lncRNAs were composed of different types of transcripts (Table 6). Four of them were anti-sense lncRNAs that overlap the genomic span of a protein-coding locus on the opposite strand. AC015849.2 has two neighboring genes, Chemokine (C-C Motif) Ligand 5 (CCL5) and TATA Box Binding Protein (TBP)-Associated Factor (TAF15). CCL5 was highly upregulated (147,688-fold), which is consistent with a previous report (70) whereas TAF15 was downregulated (5-fold). The other two anti-sense lncRNAs RP-1-7H24.1 and RP11-670E13.5 have well-known antiviral genes, OAS2, OAS3 and TRIM25 as their neighbors (71). They were also highly upregulated (Table 6). The neighboring genes of TAPSAR1, an anti-sense lncRNA; PSMB8 and TAP1 were upregulated. Neighboring genes of intergenic lincRNA CTD-2639E6.9 were either downregulated (FTL) or not detected (BAX) by RNA-seq. AC007283.5 is 3 prime overlapping lncRNA that overlaps the 3'-UTR of a protein-coding locus on the same strand and its neighboring genes, CASP10 and CFLAR were upregulated. PSOR1C3 is a sense intronic lncRNA that lies within introns and do not overlap with exons. Its neighboring genes, POU5F1 and HLA-C, were highly upregulated.

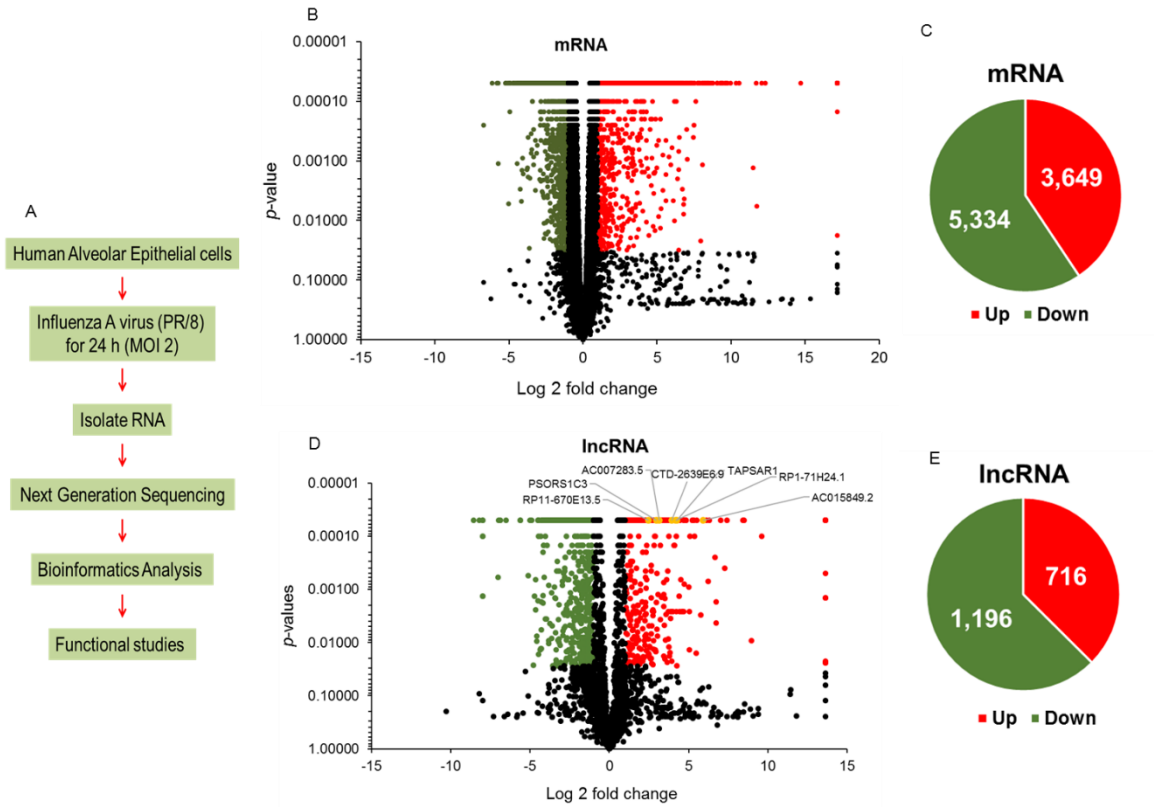

Figure 3.10. lncRNAs are differentially regulated during influenza virus infection. (A) Flowchart of RNA-seq experiment design. (B, C) Volcano plot of differentially expressed mRNAs and lncRNAs in PR/8-infected A549 cells at MOI of 2 for 24 h. Downregulated genes are denoted in green color and upregulated genes in red color based on a *p*-value of ≤ 0.05 and a fold change of ≥ 2. Genes with a *p*-value of > 0.05 or a fold change of < 2 are marked with black color. The yellow colored lncRNAs are the selected lncRNAs for further analysis (see the text). (D, E) Pie charts of significantly changed mRNAs and lncRNAs with a *p*-value of ≤ 0.05. Green and red colors denote downregulated and upregulated genes, respectively.

Table 4. Summary of RNA-seq data sets

Fold change	lncRNA		mRNA	
	Up-regulated	Down-regulated	Up-regulated	Down-regulated
> 100	68	11	80	0
50-100	5	1	45	2
10-50	71	59	238	79
2-10	274	612	1,262	2,703

Table 5. Interferon-stimulated antiviral genes

Anti-viral genes	Expression level (FPKM)		Fold change
	Control	Influenza virus	
OAS1 (2'-5'-Oligoadenylate Synthetase 1)	21	421	20
OAS2 (2'-5'-Oligoadenylate Synthetase 2)	0.12	173	1,468
OAS3 (2'-5'-Oligoadenylate Synthetase 3)	19	181	10
OASL (2'-5'-Oligoadenylate Synthetase-Like)	0.46	1,539	3,327
MX1(MX Dynamin-Like GTPase 1)	0.42	222	526
ISG15 (ISG15 Ubiquitin-Like Modifier)	3	974	367
ISG20 (Interferon Stimulated Exonuclease Gene)	6	251	41
IRF1 (Interferon Regulatory Factor 1)	9	237	27
IRF2 (Interferon Regulatory Factor 2)	9	27	3
IRF7 (Interferon Regulatory Factor 7)	2	163	74
IRF9 (Interferon Regulatory Factor 9)	39	164	4
TRIM25 (Tripartite Motif Containing 25)	27	199	7

Table 6. Selected lncRNAs and their properties

lncRNA	FPKM		Fold change	Chromosome locus	bp	Type	Neighboring genes	FPKM		Fold change
	Con	Flu						Con	Flu	
AC015849.2	8	491	60	chr17:34195970-34212867	662	anti-sense	CCL5	0.02	2,988	147,688
							TAF15	219	44	- 5
TAPSAR1	11	211	19	chr6:32811862-32814272	1,267	lincRNA	PSMB8	9	51	5
							TAP1	8	253	33
RP1-71H24.1	14	257	18	chr12:113345432-113455556	575	anti-sense	OAS2	0.12	173	1,470
							OAS3	19	181	10
CTD-2639E6.9	10	159	15	chr19:49467231-49468415	819	lincRNA	FTL	8,488	3,245	- 3
							BAX	ND	ND	ND
AC007283.5	142	1,261	9	chr2:202031687-202032269	445	3 prime overlapping	CASP10	2	14	6
							CFLAR	27	137	5
PSORS1C3	31	245	8	chr6:31141511-31145676	593	Sense intronic	POU5F1	2	22	13
							HLA-C	24	412	17
RP11-670E13.5	337	1,880	6	chr17:54966240-54969202	538	anti-sense	TRIM25	27	199	7
							DGKE	ND	ND	ND

Fold changes: from RNA-seq data
bp: length in terms of base pairs
ND: Not detected by RNA-seq
- number: Downregulation
FPKM: Fragments Per Kilo base of transcript per Million mapped reads
CCL5: Chemokine (C-C motif) ligand 5
TAF15: TATA Box Binding Protein (TBP)-Associated Factor
PSMB8: Proteasome Subunit Beta 8
TAP1: Transporter 1, ATP-Binding Cassette
OAS2: 2'-5'-Oligoadenylate Synthetase 2
OAS3: 2'-5'-Oligoadenylate Synthetase 3
FTL: Ferritin, Light Polypeptide
BAX: BCL2-Associated X Protein
CASP10: Caspase 10, Apoptosis-Related Cysteine Peptidase
CFLAR: CASP8 and FADD-Like Apoptosis Regulator
POU5F1: POU Class 5 Homeobox 1
HLA-C: Major Histocompatibility Complex, Class I, C
TRIM25: Tripartite Motif Containing 25
DGKE: Diacylglycerol Kinase, Epsilon

3.12 Go pathway analysis of lncRNAs

Because the functions of most lncRNAs are unknown and lncRNAs often regulate their neighboring genes (72) , we selected the genes within 10,000 kb of significantly changed lncRNAs during influenza virus infection for GO analysis including cellular components, molecular pathways and biological processes. Prediction terms with a p-value of less than 0.05 were selected and ranked. Enrichment scores (−log10(p-value) were plotted on x-axis. The most enriched cellular components were related to endosome (Fig. 3.11A). The genes involved in the α, β, and γ IFN and immune signaling or cellular responses are enriched in the molecular and biological pathways (Fig. 3.11B, C). The GO analysis revealed the neighboring genes of the lncRNAs changed by influenza virus were enriched in the pathways and processes that are known to be involved in influenza virus infection.

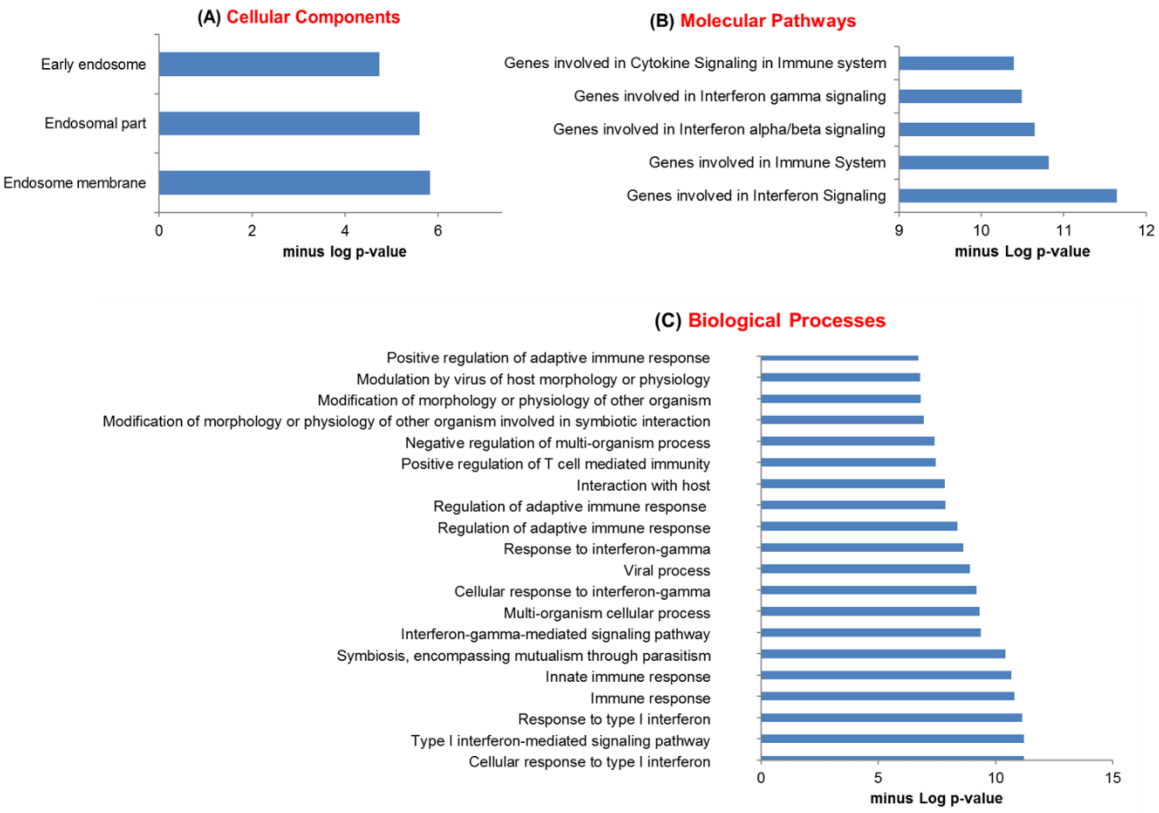

Figure 3.11. GO pathway analysis of lncRNA co-expressed mRNAs. Protein-coding genes within 10,000 kb distance of the significantly dysregulated lncRNAs during influenza virus infection were selected for GO analysis. GO analysis includes 3 annotations- cellular components (A), molecular pathways (B) and biological process (C). GO id with a *p*-value of < 0.05 were selected**.**

3.13 Validation of RNA-seq results with qPCR

We then utilized real-time PCR to validate the results from RNA-seq analysis using the same RNAs from the RNA-seq analysis. Real-time PCR confirmed that all of the 7 lncRNAs were induced by PR/8 (Fig. 3.12A) although the absolute fold changes varied between real-time PCR and RNA-seq for some lncRNAs (Fig. 3.12C). For the mRNA real-time PCR validation, we selected the genes that are implicated in endoplasmic reticulum (ER) stress since ER stress is involved in viral replication and *vice-versa* (73, 74). The genes that were included for this analysis were UDP-Glucose Glycoprotein Glucosyltransferase 2 (UGGT2), Ubiquitin-Conjugating Enzyme E2G 2 (UBE2G2), Glucosidase, Alpha; Neutral AB (GANAB), BCL2-Associated Athanogene 2 (BAG2), SIL1 Nucleotide Exchange Factor (SIL1), Eukaryotic translation initiation factor 2-alpha kinase 1 (ELF2AK1) and Ubiquitination Factor E4B (UBE4B). All of the genes were down-regulated and similar changes were observed using real-time PCR and RNA-seq (Fig. 3.12B, D).

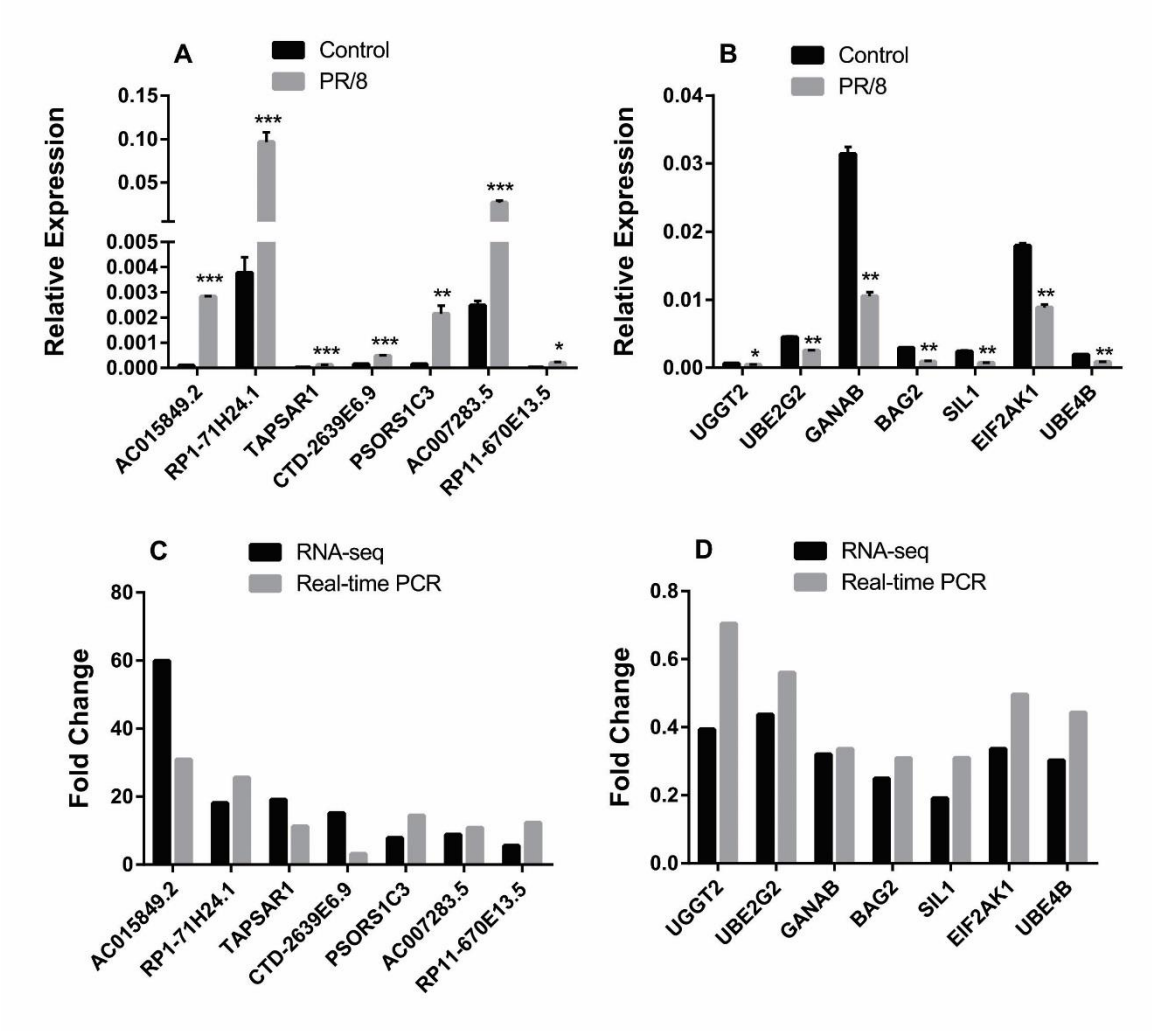

Figure 3.12. Real-time PCR confirmation of RNA-seq results. (A, B) Relative expression of selected lncRNAs and mRNAs performed on the same samples as for RNA-seq using real-time PCR. Data was normalized to β-actin and expressed as means ± SE. n = 3 independent experiments. *$p < 0.05$, **$p < 0.01$, and ***$p < 0.001$ vs. control (paired student's t-test). (C, D) Comparison of fold changes between RNA-seq and real-time PCR

3.14 Effects of influenza virus strains on lncRNA expression

Influenza A virus strains exhibit different virulence for a particular host (75). We thus examined if the up-regulated lncRNAs by PR/8 are also induced by other strains of influenza viruses. We found that lncRNA induction by PR/8 is dose-dependent (Fig. 3.13). RP1-7H24.1, TAPSAR1, and RP11-670E13.5 expression reached maximum at a MOI of 0.2 while AC015849.2, CTD-2639E6.9, AC007283.5, and PSORS1C3 had a highest expression at a MOI of 2. We then compared the effects of 3 influenza A virus strains on the lncRNA expression using a MOI of 2 in A549 cells: PR/8, WSN and Pdm/OK. WSN and Pdm/Ok are another commonly used laboratory strain and a clinical isolate of 2009 Oklahoma pandemic influenza H1N1 virus of swine origin, respectively. All of the seven lncRNAs were induced by all the strains except that Pdm/OK had no effects on PSORS1C3 expression and that Pdm/Ok-induced RP11-670E13.5 expressions did not reach a significant level due to the variation between the experiments (Fig. 3.13). However, the magnitude of induction varied among strains and lncRNAs. Similar inductions were observed for TAPSAR1 by 3 strains. WSN induced much higher expression of AC015849.2, CTD-2639E6.9 and PSORS1C3 compared to PR/8 and Pdm/OK while PR/8 and Pdm/OK increased RP1-7H24.1expression more than WSN. PR/8 and WSN were more effective in the induction of AC007283.5 than Pdm/OK. Finally, PR/8 induced a higher expression of RP11-670E13.5 than WSN.

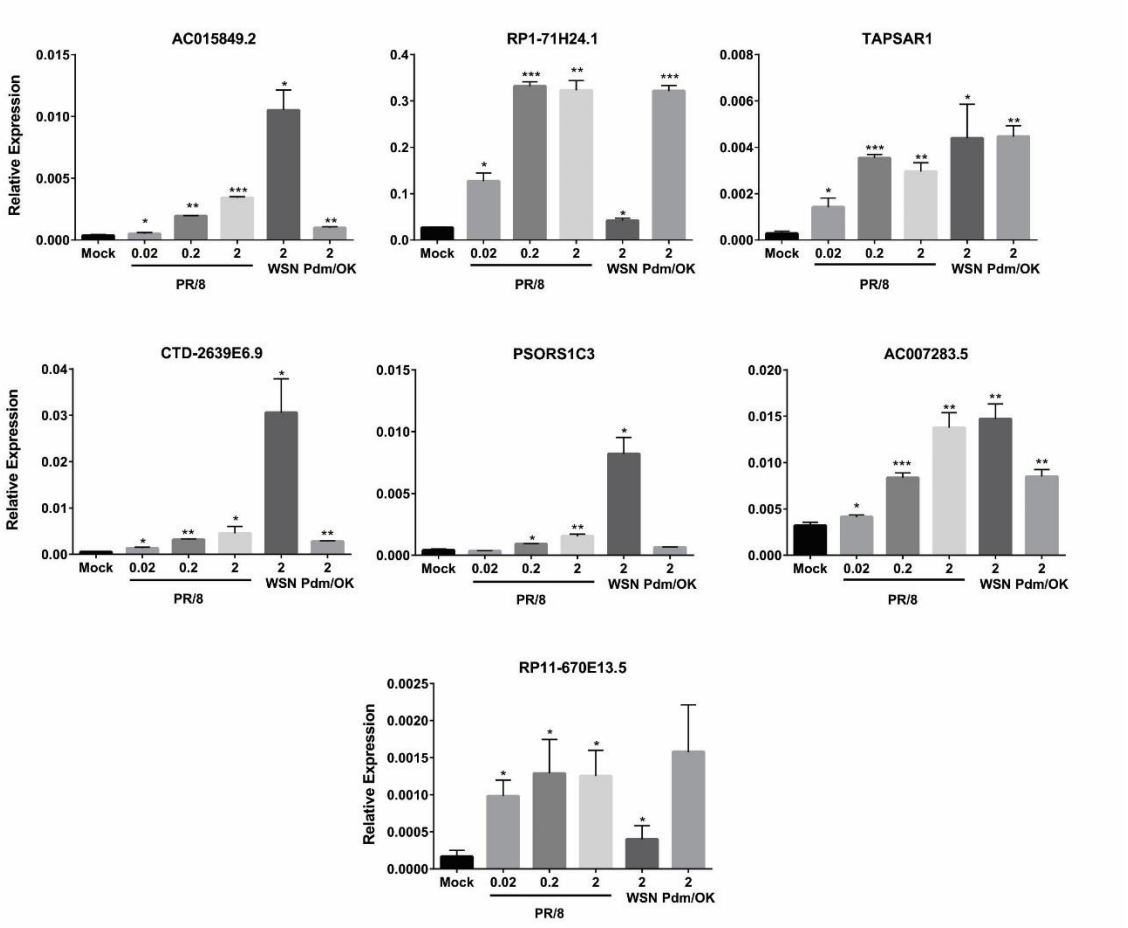

Figure 3.13. lncRNA induction by different influenza viruses. A549 cells were infected with influenza A viruses, PR/8 (MOI: 0.02, 0.2 and 2), WSN (MOI 2) and Pdm/OK (MOI 2) for 24 h. lncRNA expression levels were determined by real-time PCR and normalized to β-actin. Results are represented as means ± SE from three independent experiments. *$p < 0.05$, **$p < 0.01$ and ***$p < 0.001$ vs. mock control (Student's t-test)

3.15 lncRNAs are induced by IFNβ1

Influenza viruses are known to induce IFN response. Hence, we examined whether type I IFN induce the expression of lncRNAs identified above. We treated A549 cells with 1,000 U/ml IFNβ1 for different times (0, 3, 9 and 24 h) and determined the expression levels of lncRNAs by real-time PCR. IFNβ1 treatment markedly increased the expression of OAS1, a known ISG gene (76) (Fig. 3.14). We found that 6 of the 7 lncRNAs were significantly induced by IFNβ1. PSORS1C3 level was also increased by IFNβ1, but did not reach a significant level. The IFNβ1-induced expression of lncRNAs occurred as early as 3 h post treatment and reached a maximum at 3 h for AC007283.5, RP11-670E13.5 and TAPSAR1, 9 h for RP1-71H24.1 and 24 h for AC015849.2.

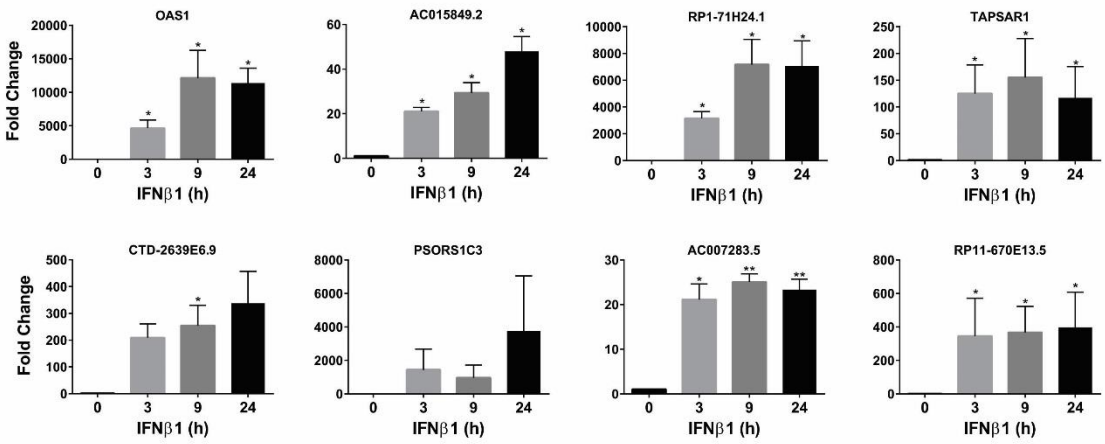

Figure 3.14 Effect of IFNβ1 on lncRNA expression. A549 cells were treated with IFNβ1a (1,000 U/ml) for different times. Interferon inducible gene, OAS1 and lncRNA levels All 7 were determined by real-time PCR and normalized to18S rRNA. Fold change was calculated based on 0 h and results are represented as means ± SE from three independent experiments. *$p < 0.05$, and **$p < 0.01$ vs. 0 h (Student's t-test)

3.16 Knockdown of lncRNAs using lentivirus shRNAs

To determine the functional roles of the identified lncRNAs on influenza virus replication we attempted to knockdown lncRNAs using lentivirus-based shRNAs. The expression levels of TAPSAR1, CTD-2639E6.9, and PSORS1C3 were reduced by 52.07 ± 0.92, 48.06 ± 2.73 and 43.3.3 ± 3.8% by TAPSAR1 shRNA-1, CTD-2639E6.9 shRNA-2 and PSORS1C3 shRNA-3 respectively (Fig.3.15B).

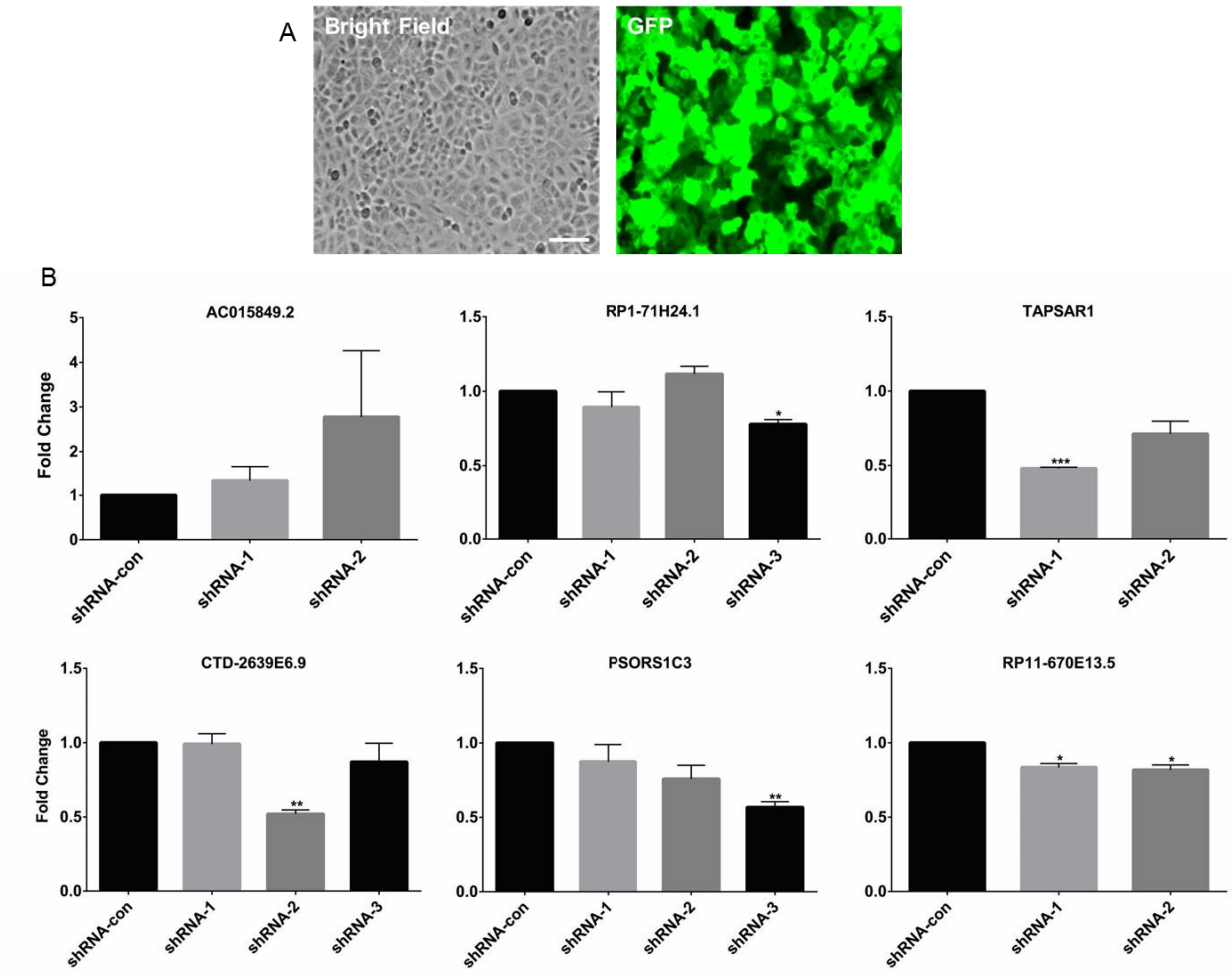

Figure 3.15. Knockdown efficiency of lncRNA shRNAs. A549 cells were infected with a lentiviral lncRNA shRNA or its control (shRNA-Con) at a MOI of 100 for 48 h, followed by PR/8 infection at a MOI of 2 for 24 h. LncRNA shRNA infection efficiency was monitored by GFP (A) and representative images of shRNA-con were shown in A (Scale bar = 50 μm). LncRNA knockdown (B) efficiency was measured by real-time PCR and β-actin was used as a housekeeping control. Fold change was calculated based on shRNA-con. Results are represented as means ± SE from three independent experiments. *$p < 0.05$, and **$p < 0.01$ vs. shRNA-Con (Student's t-test).

3.17 Knockdown of TAPSAR1 reduces influenza virus replication

We then determined the effects of TAPSAR1, CTD-2639E6.9 and PSORS1C3 knockdown on influenza virus replication. The virus titer in the culture medium of TAPSAR1 shRNA-1-treated cells was reduced 10-fold compared to shRNA-control (Fig. 3.16). We did not observe significant reduction in the virus titer with knockdown of other two lncRNAs CTD-2639E6.9 and PSORS1C3 with the shRNAs which were able to knockdown respective lncRNA (Fig. 3.15B).

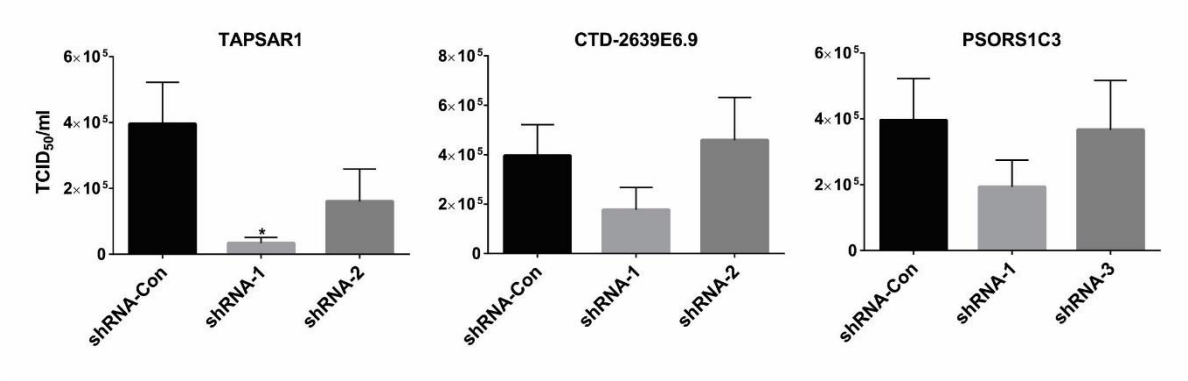

Figure 3.16 Effect of lncRNA knockdown on influenza virus replication. A549 cells were infected with lentiviral shRNA-Con or shRNA against TAPSAR1, CTD-2639E6.9 and PSORS1C3 at a MOI of 100 for 48 h, followed by PR/8 infection at a MOI of 2 for 24 h. Influenza virus particles in culture media were determined by $TCID_{50}$ assay in MDCK cells. Results are expressed as $TCID_{50}$/ml and represented as means ± SE from three independent experiments. *$p < 0.05$ vs. shRNA-Con (Student's t-test).

3.18 TAPSAR1 knockdown results in reduced influenza viral protein synthesis and mRNA.

We further investigated the effects of TAPSAR1 knockdown on influenza viral mRNA and protein levels in single-cycle and multi-cycle infections. We knocked down TAPSAR1 in A549 cells with TAPSAR1 shRNA-1 for 48 h and infected with PR/8 at MOI 2 for 8 h (single-cycle) or MOI 0.2 for 24 h (multi-cycle). The reduction of TAPSAR1 levels were confirmed in both types of infection cycle settings (Fig. 3.17A). The knockdown of TAPSAR1 significantly reduced NS1 protein levels in both single-cycle and multi-cycle infections (Fig. 3.17B, C). Matrix protein 2 (M2) and nuclear protein (NP) were significantly decreased by TAPSAR1 knockdown in single-cycle and multi-cycle infections, respectively (Fig. 3.17B, D, E). TAPSAR1 shRNA2, which did not decrease the TAPSAR1 level, had no effects on influenza viral protein expression. The knockdown of TAPSAR1 had no effects on mRNA levels of NS1, M2 and NP in single-cycle and multi-cycle infection except NP mRNA was moderately reduced in single-cycle infection (Fig. 3.18C)**.** Taken together, these results indicate that TAPSAR1 knockdown mainly affects late stage of influenza virus replication cycle after mRNA synthesis.

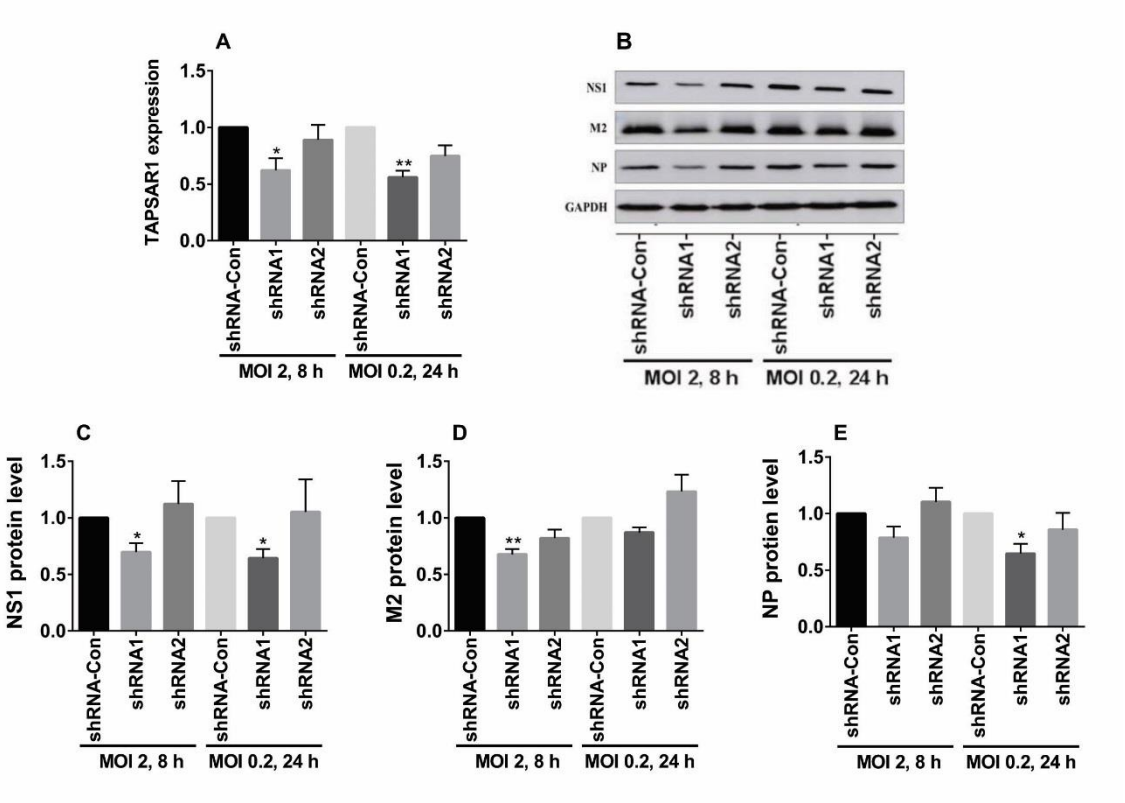

Figure 3.17 Effect of TAPSAR1 knockdown on influenza virus protein synthesis. A549 cells were infected with lentiviral shRNA-Con or shRNA against TAPSAR1 at a MOI of 100 for 48 h, followed by PR/8 infection at a MOI of 2 for 8 h (single-cycle infection) or at a MOI of 0.2 for 24 h (multi-cycle infection). (A) TAPSAR1 expression levels were determined by real-time PCR and normalized to β-actin. (B-E) Influenza viral protein (NS1, M2 and NP) levels were measured by western blotting. The protein bands were quantitated using Image Quant software and normalized to GAPDH. All of the data are expressed as a fold change over respective shRNA-Con and represented as means ± SE from 3 independent experiments. *$p < 0.05$ vs. respective shRNA-Con, **$p < 0.01$ vs. respective shRNA-Con (Student's t-test)

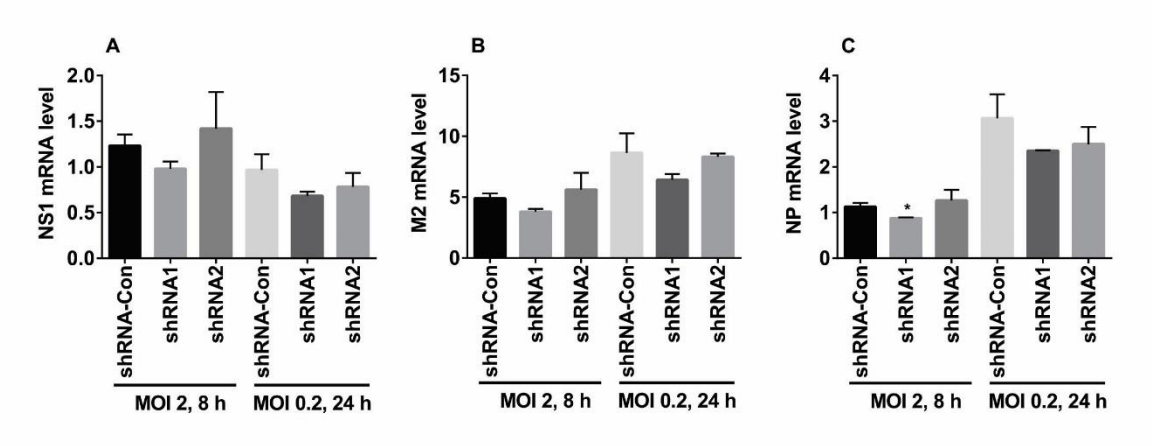

Figure 3.18 Effects of TAPSAR1 knockdown on influenza virus mRNAs. A549 cells were infected with lentiviral shRNA-Con or shRNA against TAPSAR1 at a MOI of 100 for 48 h, followed by PR/8 infection at a MOI of 2 for 8 h (single-cycle infection) or at a MOI of 0.2 for 24 h (multi-cycle infection). mRNA levels of NS1 (A), M2 (B) and NP (C) were measured by real-time PCR and normalized with β-actin. Data is represented as means ± SE from 3 independent experiments. *$p < 0.05$ vs. shRNA-Con (Student's t-test).

3.19 TAPSAR1 is localized in nucleus of A549 cells

As the first step in elucidating mechanisms of TAPSAR1-mediated influenza virus replication, we determined the location of TAPSAR1 in cells. We isolated cytoplasmic and nuclear fractions from A549 cells and determined TAPSAR1 levels in both fractions using real-time PCR. As shown in Fig. 3.19, TAPSAR1 was enriched in the nucleus similar to nuclear U2snRNA. Cytoplasmic β-actin and GAPDH mRNAs were primarily located in the cytoplasm.

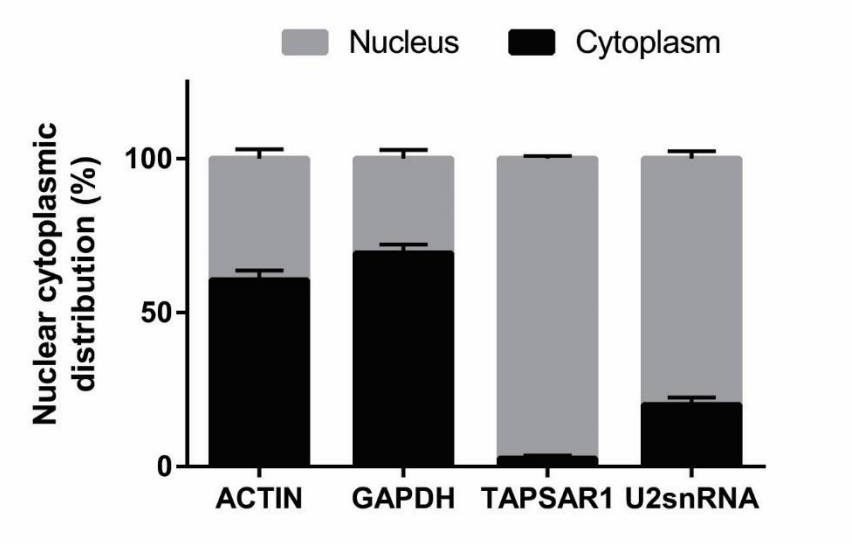

Figure 3.19. Location of TAPSAR1 in A549 cells. The levels of TAPSAR1, GAPDH and β-actin mRNAs (cytoplasmic RNA positive controls), and U2snRNA (nuclear RNA positive control) in cytoplasmic and nuclear fractions of A549 cells were determined by real-time PCR. Results are represented for each gene as means ± SE from three independent experiments.

3.20 Knockdown of TAPSAR1 does not affect its neighboring gene PSMB8

Human TAPSAR1 is located on chromosome 6p21.32 and overlapping with the antisense strand of TAP1 (Transporter 1, ATP-Binding Cassette, Sub-Family B protein) and PSMB8 (Proteasome Subunit, Beta Type, 8) genes. TAP1 is involved in the transport of antigens from the cytoplasm to the endoplasmic reticulum for association with MHC class I molecule (77), whereas PSMB8 plays role in antigen processing to generate class I binding peptides (78). Because lncRNAs may function by regulating their neighboring genes, we evaluated mRNA expression of TAP1 and PSMB8 after the knockdown of TAPSAR1 in A549 cells. TAPSAR1 shRNA-1 reduced the TAPSAR1 level by 52 % and TAPSAR1 shRNA-2 had no significant effects on TAPSAR1 expression (Fig. 3.15B). However, both TAPSAR1 shRNA-1 and shRNA-2 did not affect PSMB8 mRNA expression (Fig. 3.20). TAP1 mRNAs were not detectable in all the conditions. This result suggests that the effects of TAPSAR1 on influenza virus infection are unlikely through a *cis*-effect on TAP1 and PSMB8 genes.

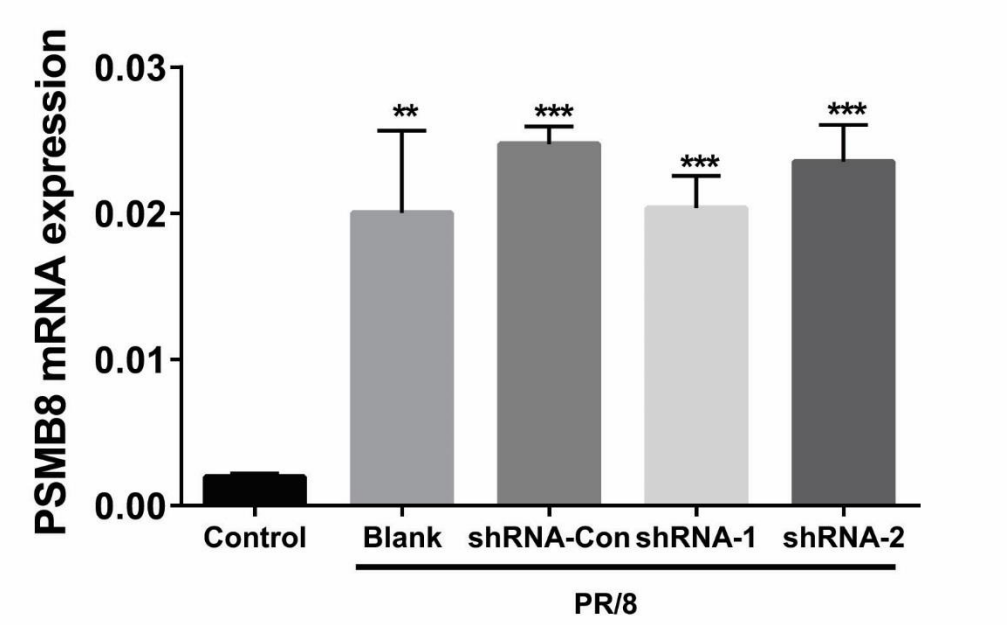

Figure 3.20. Effects of TAPSAR1 knockdown on PSMB8 expression. Real-time PCR analysis of PSMB8 mRNA in A549 cells infected with lentivirus for 48 h with shRNA-con, shRNA-1and shRNA-2 followed by PR/8 infection at MOI 2 for 24 h. A549 cells with (Blank) or without (Control) at same MOI of PR/8 served as controls. PSMB8 levels were measured by real-time PCR and normalized to β-actin. Results are represented as mean ± SE from three independent experiments $^{**}p < 0.01$ and $^{***}p < 0.001$ vs. Control (Student's t-test)

3.21 TAPSAR1 knockdown results in the reduction of IP10

To screen potential antiviral genes that are changed by TAPSAR1 knockdown, we performed real-time PCR for OAS1, OAS2, ISG56, TLR7, IL6 and IP10. TAPSAR1 knockdown had no effects on OAS1, OAS2, ISG56 and IL6 expression, but significantly reduced TLR7 and IP10 level (Fig. 3.21).

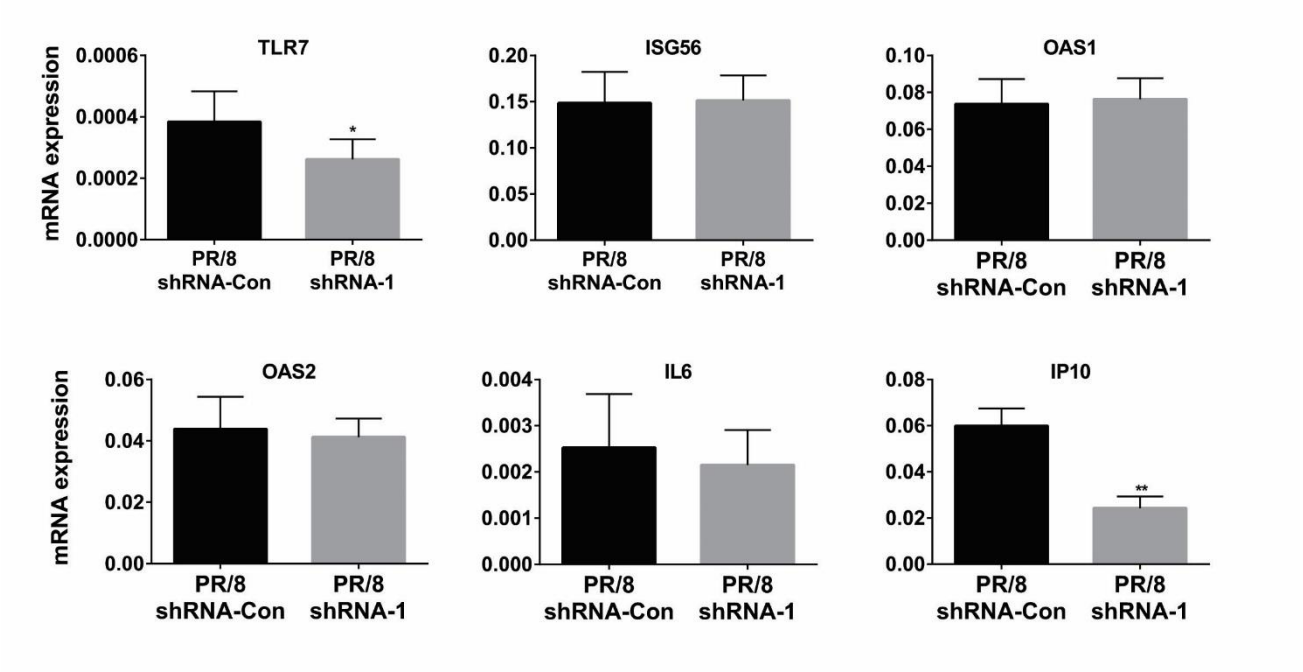

Figure 3.21. Antiviral response gene profiles after TAPSAR1 knockdown. A549 cells were infected with lentiviral shRNA-Con or shRNA1 against TAPSAR1 at a MOI of 100 for 48 h, followed by PR/8 infection at a MOI of 2 for 8 h. Real-time PCR analysis of antiviral genes and inflammatory cytokines using 3 independent shRNA-Con and 3 shRNA1 samples. The results were normalized to β-actin. Data is represented as means ± SE from three independent experiments. *$p < 0.05$ and **$p < 0.01$ vs. shRNA-Con (Student's t-test).

CHAPTER IV

DISCUSSION

4.1 Influenza virus and host signaling pathways.

In this study, we found that activation of Wnt/β-catenin with Wnt3a enhanced influenza virus replication and that inhibition of this pathway with iCRT14 decreased influenza virus transcription and production of new virus. iCRT14 acted at or before viral RNA synthesis and its effect was independent of IFN production. iCRT14 also showed a partial protective effect in a mouse model of influenza virus infection and may have potential for development as a therapeutic candidate against influenza virus.

Various host signaling pathways are altered during influenza virus infection and thus these pathways can provide potential therapeutic targets. Cellular signaling pathways such as NF-κB signaling, MAPK pathway, PI3K/Akt pathway, PKC/PKR signaling, and TLR/RIG-I signaling cascades have been reported to play role in various stages of the influenza virus replication cycle. NF-κB signaling is essential for the host innate immune response and is activated by influenza virus infection (79). Once it is activated, NF-κB signaling increases influenza virus production by inducing proapoptotic factors (80). Influenza virus also activates the MAPK pathway and blocking this signaling pathway inhibits virus replication by impairing viral ribonucleoprotein trafficking (81). Another pathway that is activated by influenza virus is

the PI3K/Akt pathway via the interaction of NS1 and p85β (82). There is robust activation of interferon response during influenza virus infection, which in turn activates the PKR signaling pathway. However, influenza virus also counteracts activation of PKR pathway by the binding of NS1 to double stranded RNA, thereby preventing translational arrest (83). Pattern recognition receptors such as toll-like-receptors (TLR) and RIG-I like receptors (RLRs) recognize viral RNAs and induce antiviral immune responses (84). Influenza virus has also evolved mechanisms to counteract this induction of the antiviral response. For example, NS1 inhibits RIG-I activation and IFN production by binding TRIM25, an ubiquitin ligase that is required for RIG-I activation (85).

4.2 Wnt signaling and influenza virus

Our current study demonstrates that Wnt/β-catenin signaling enhances influenza virus replication as we showed that Wnt3a enhanced viral gene expression in PR8-infected mouse lung epithelial cells in cell culture and PR8-infected lungs in vivo. We also demonstrated that the Wnt/β-catenin inhibitor, iCRT14 inhibited virus replication and viral gene expression in H1N1 A/PR/8/34- and A/WSN/33-infected human lung epithelial A549 cells and primary mouse alveolar epithelial cells. There are very limited studies on the effects of Wnt/β-catenin signaling on influenza virus infection. Using an RNAi approach, one study has reported that silencing of various components in Wnt/β-catenin signaling affects PR8 replication. However, the results are difficult to interpret since the deletion of these genes has either a positive or negative effect on PR8 replication (13). Another study has shown that the addition of Wnt3a or overexpression of β-catenin inhibits H7N7 influenza virus replication (86), in contrast with our observation that Wnt3a actually enhances H1N1 viral gene expression. The discrepancy is likely due to the difference in strains and/or cells used.

4.3 iCRT14 and interferon response

The inhibition of influenza virus replication by iCRT14 is not via the IFN response since iCRT14 maintained its ability to inhibit influenza virus replication in the IFN-deficient Vero cells and had no effects on the influenza virus-induced IFN response in A549 cells. Different effects of Wnt/β-catenin on IFN response during virus infection were reported. The Wnt ligand WNT2B and WNT9B negatively regulate the IFN response during Sendai virus infection (87) and deletion of WNT9B positively regulates the IFN response (13). In contrast, Wnt3a increases the IFN response in the absence of NS1 protein, which is the main protein that influenza virus uses to repress the host IFN response (13). The transfection of β-catenin and LEF-1 plasmids into A549 cells also induces the ISRE gene reporter when treated with cellular or viral RNA (86).

4.4 iCRT14 and *in vivo* studies

In a xenograft model of BT-474 cells in SCID mice, iCRT14 treatment was shown to reduce tumor volume significantly (67). Mouse Ewing's sarcoma *in vivo* was also inhibited by iCRT14 (88). However, there is a paucity of literature on the toxicity of iCRT14 in animals. Our 10-day toxicity study in mice did not reveal any major toxicity in organs such as lung, liver, kidney, brain, heart and eyes. In a sub-lethal influenza infection mouse model, iCRT14-treated mice showed less severe clinical symptoms, which were correlated with the observation that those mice had lower virus loads (Fig. 3.8A). Influenza virus infection causes acute lung injury including damage to endothelial and epithelial cells, disruption of the endothelial alveolar barrier, leakage of proteins into the alveolar space, and inflammatory cell infiltration. However, iCRT14 appears to have no effects on parameters of lung injury and inflammation except that it reduces lung edema. In a lethal influenza infection, we only observed slightly lower weight loss and delayed mortality in iCRT14-treated mice. These end points could be used to improve the efficacy of iCRT14 with medicinal chemistry and formulation. Since iCRT14 reduced virus loads

and improved clinical symptoms, a combination therapy (89) with other drugs to reduce lung injury should increase efficacy of iCRT14.

4.5 RNA-seq experiment

Influenza virus requires host cellular factors to function as revealed by several high throughput and genome wide studies (90-92). Since virus infection leads to global translation inhibition (93), a translation-independent system is needed to prepare cells for antiviral responses. lncRNAs represent a such potential class of host factors and are new alternatives for development of host-centric antiviral strategies. In this study we identified a lncRNA TAPSAR1 whose knockdown reduced influenza virus replication. TAPSAR1 was induced by different influenza virus strains and type I IFN. TAPSAR1 knockdown led to reduction in proinflammatory cytokine IP10.

Our present studies showed that a large number of human lncRNAs (3,158), along with protein-coding genes (8,638), were differentially expressed after influenza virus infection. A recent microarray analysis reported a similar number of non-coding transcripts (3,415 and 3,401) altered by influenza virus infection using two commercial microarrays, NCode™ and Sureprint™ G3 (50). However, RNA-seq technique yields more comprehensive datasets of both lncRNA and mRNA along with less false-positive hits (94).

It is well known that influenza virus hijacks cellular protein synthesis machinery (95) to make more viral proteins. It is conceivable that many of the cellular mRNAs are downregulated (96). Our RNA-seq datasets revealed a higher number of lncRNAs and mRNAs were up-regulated than these that were down-regulated. Previous studies have shown that lncRNAs can regulate their neighboring genes (72). GO analysis using upstream and downstream protein coding genes within 10,000 kb distance of the dysregulated lncRNAs indicated that many of the lncRNAs were associated with pathogen-related immune signaling pathways and responses based on molecular pathway and biological process analysis and endosomes based on cellular

component enrichment. This is consistent with the fact that influenza virus enters cells via endocytosis (97). Thus there is a correlation between influenza virus infection and the pathways and processes that are highly enriched for immune signaling and responses.

4.6 LncRNAs and viruses

Among 1,298 up-regulated lncRNAs in PR/8-infected cells, 7 selected lncRNAs in our studies were also induced by other H1N1 strains, WSN and Pdm/OK, but the magnitude of induction varied, indicating that there are differences in virus strains in induction of lncRNA expression. lncRNA expression can be induced by not only influenza viruses but also other RNA viruses including human immunodeficiency virus (HIV) (45) and hepatitis C virus (HCV) (49) and DNA viruses such as herpesviruses (46). Efforts have been made to understand if lncRNA induction is due to a direct viral effect or changes in host cellular signaling. One study has demonstrated that live influenza virus is necessary for induction of lncRNA VIN (50). Although it is induced by various strains of influenza virus such as H1N1, H3N2 and H7N7, VIN is not inducible by IFN or viral RNA mimics. On other hand, host IFN signaling also contribute to the induction of lncRNA expression as demonstrated by using IFNs (52, 98, 99) or NS1-mutant virus which is unable to counteract IFN response from host (100). The seven lncRNAs used in our studies were also induced by type I IFN.

4.7 Function of TAPSAR1

Functional analysis of one of the highly upregulated lncRNA TAPSAR1 indicated that it acts as pro-viral for influenza virus replication. LncRNAs NRAV (48) and VIN (100) have been shown to reduce virus replication. VIN is required for influenza virus replication and its deletion reduces virus yield and protein synthesis however the exact mechanism is yet to be clarified. NRAV is involved in the downregulation of Mx1 and interferon induced transmembrane protein 3 (IFITM3) through histone modification of these genes which are crucial to anti-viral immune

response during influenza virus infection. TAPSAR1 knockdown led to the reduction in virus titer and protein synthesis but had almost no effect on viral mRNA translation or protein stability. This suggests that TAPSAR1 may be involved in late stages of virus replication such as synthesis and/or export of virus proteins.

4.8 LncRNA location and neighbouring genes

Localization of lncRNAs in cells may provide significant information about how their functions are achieved. lncRNA in the cytoplasm such as DANCR can compete for miRNA binding sites (101). lncRNAs in the nucleus can regulate gene transcription through chromatin modification (102). NEAT1 and MALAT1 are present in paraspeckles and nuclear speckles inside the nucleus, respectively (51) (103). NEAT1 is responsible for maintaining structure of paraspeckles (104) as well as regulation of transcription of IL-8 genes (51). MALAT1 is known to regulate genes associated with lung cancer metastasis (105). Another nuclear lncRNA, NRAV functions as a histone modification factor of anti-viral genes, MxA and IFITM3 (48) TAPSAR1 is predominantly located in the nucleus of A549 cells which suggest that it may play a role in transcription, chromatin remodeling or post-transcriptional processing (106). However, exact role and location inside the nucleus of TAPSAR1 during influenza virus infection remains to be determined.

Human TAPSAR1 has two neighboring genes, TAP1 and PSMB8. Even though PSMB8 was induced by PR/8, we did not observe any significant changes in PSMB8 level after knockdown of TAPSAR1. We could not detect TAP1 in control or PR/8-infected lung epithelial A549 cells using real-time PCR. TAP1 and PSMB8 have previously been shown to be induced by influenza virus (107, 108) and other viruses (109, 110).

4.9 IP10 in influenza virus infection

Our present studies showed that the reduction of TAPSAR1 level by 38% resulted in 60% decrease in IP10 expression in PR/8-infected A549 cells. IP10 also called C-X-C motif chemokine 10 (CXCL10) is an interferon-γ that functions in monocyte stimulation, natural killer and activated T cell migration (111). IP10 induction is critical for a proper adaptive immune response to promote inflammation and recruit lymphocytes to the site of infection. Although neutrophils have been identified as a source of IP10 (112, 113) during influenza virus-induced respiratory syndrome, influenza H1N1 virus induces a high level of IP10 in human lung epithelial cells (114-116) and human lung slice culture (117). Mortality caused by influenza virus is largely associated with cytokine storm due to hyperactivation of immune system (118). Higher levels of IP10 in the serum of 2009 swine-origin influenza virus infected patients was observed (119). A high level of IP10 and other pro-inflammatory cytokine mRNAs was correlated to acute lung injury (114) whereas lower levels of IP10 have been correlated to hepatitis C virus clearance (120). It has been also shown that IP10 stimulates HIV replication (121). The gene deletion or antibody neutralization of IP10 protects the mice from influenza virus infection (119). CXCR3 is a receptor for IP10 and its deletion also improves the severity of influenza virus–induced lung injury (112). We speculate that TAPSAR1 involvement in influenza virus replication may be mediated through IP10 and further studies are needed to support this speculation.

CHAPTER V

CONCLUSIONS

5.1 Wnt signaling inhibitor iCRT14 and influenza virus

Present study provides evidence that inhibition of Wnt/β-catenin signaling limits influenza virus infection by reducing influenza virus replication independent of the IFN response. Inhibitor of this pathway iCRT14 was able to inhibit the RNA synthesis of influenza virus. ICRT14 was also able to successfully inhibit virus replication of two different strains of influenza virus in primary alveolar epithelia cells. Wnt/β-catenin inhibitors may be used to develop a new class of antivirals targeting host factors.

5.2 iCRT14 protects mice from influenza virus infection

Wnt3a conditional media increased influenza virus replication in mice. iCRT14 partially protects mice from lethal and sub-lethal influenza virus challenges. Histopathology related to influenza virus induced-pneumonia was also partially attenuated by iCRT14.

5.3 LncRNA and influenza virus

LncRNA were dysregulated by influenza virus infection as revealed by RNA-seq approach. Some lncRNA expression was also induced by different influenza virus strains and type I interferon. GO analysis of neighbouring genes of dys-regulated lncRNAs suggest that the

pathways related to immune signaling, cellular components and biological processes were highly involved.

5.4 Effect of lncRNA TAPSAR1 knockdown on influenza virus replication.

The knockdown of lncRNA TAPSAR1 inhibited influenza virus replication and reduced the proinflammatory cytokine IP10 expression.

REFERENCES

1. **Matsuoka Y, Matsumae H, Katoh M, Eisfeld AJ, Neumann G, Hase T, Ghosh S, Shoemaker JE, Lopes TJ, Watanabe T, Watanabe S, Fukuyama S, Kitano H, Kawaoka Y.** 2013. A comprehensive map of the influenza A virus replication cycle. BMC systems biology **7:**97.
2. **Bouvier NM, Palese P.** 2008. The biology of influenza viruses. Vaccine **26 Suppl 4:**D49-53.
3. **Ferguson NM, Galvani AP, Bush RM.** 2003. Ecological and immunological determinants of influenza evolution. Nature **422:**428-433.
4. **Thompson WW, Shay DK, Weintraub E, Brammer L, Cox N, Anderson LJ, Fukuda K.** 2003. Mortality associated with influenza and respiratory syncytial virus in the United States. Jama **289:**179-186.
5. **Noah DL, Noah JW.** 2013. Adapting global influenza management strategies to address emerging viruses. American journal of physiology. Lung cellular and molecular physiology **305:**L108-117.
6. **Kelso JK, Halder N, Milne GJ.** 2013. Vaccination strategies for future influenza pandemics: a severity-based cost effectiveness analysis. BMC infectious diseases **13:**81.
7. **Hayden FG, Hay AJ.** 1992. Emergence and transmission of influenza A viruses resistant to amantadine and rimantadine. Current topics in microbiology and immunology **176:**119-130.

8. **Aeffner F, Bratasz A, Flano E, Powell KA, Davis IC.** 2012. Postinfection A77-1726 treatment improves cardiopulmonary function in H1N1 influenza-infected mice. American journal of respiratory cell and molecular biology **47:**543-551.

9. **Tarbet EB, Vollmer AH, Hurst BL, Barnard DL, Furuta Y, Smee DF.** 2014. In vitro activity of favipiravir and neuraminidase inhibitor combinations against oseltamivir-sensitive and oseltamivir-resistant pandemic influenza A (H1N1) virus. Archives of virology **159:**1279-1291.

10. **Furuta Y, Gowen BB, Takahashi K, Shiraki K, Smee DF, Barnard DL.** 2013. Favipiravir (T-705), a novel viral RNA polymerase inhibitor. Antiviral research **100:**446-454.

11. **Cao RY, Xiao JH, Cao B, Li S, Kumaki Y, Zhong W.** 2013. Inhibition of novel reassortant avian influenza H7N9 virus infection in vitro with three antiviral drugs, oseltamivir, peramivir and favipiravir. Antiviral chemistry & chemotherapy.

12. **Martinez-Gil L, Alamares-Sapuay JG, Ramana Reddy MV, Goff PH, Premkumar Reddy E, Palese P.** 2013. A small molecule multi-kinase inhibitor reduces influenza A virus replication by restricting viral RNA synthesis. Antiviral research **100:**29-37.

13. **Shapira SD, Gat-Viks I, Shum BO, Dricot A, de Grace MM, Wu L, Gupta PB, Hao T, Silver SJ, Root DE, Hill DE, Regev A, Hacohen N.** 2009. A physical and regulatory map of host-influenza interactions reveals pathways in H1N1 infection. Cell **139:**1255-1267.

14. **Song L, Liu H, Gao S, Jiang W, Huang W.** 2010. Cellular microRNAs inhibit replication of the H1N1 influenza A virus in infected cells. Journal of virology **84:**8849-8860.

15. **Anastas JN, Moon RT.** 2013. WNT signalling pathways as therapeutic targets in cancer. Nat Rev Cancer **13:**11-26.

16. **Gonsalves FC, Klein K, Carson BB, Katz S, Ekas LA, Evans S, Nagourney R, Cardozo T, Brown AM, DasGupta R.** 2011. An RNAi-based chemical genetic screen identifies three small-molecule inhibitors of the Wnt/wingless signaling pathway. Proceedings of the National Academy of Sciences of the United States of America **108:**5954-5963.

17. **Weiser K, Barton M, Gershoony D, Dasgupta R, Cardozo T.** 2013. HIV's Nef interacts with beta-catenin of the Wnt signaling pathway in HEK293 cells. PloS one **8:**e77865.

18. **Liu J, Wang Z, Tang J, Tang R, Shan X, Zhang W, Chen Q, Zhou F, Chen K, Huang A, Tang N.** 2011. Hepatitis C virus core protein activates Wnt/beta-catenin signaling through multiple regulation of upstream molecules in the SMMC-7721 cell line. Archives of virology **156:**1013-1023.

19. **Street A, Macdonald A, McCormick C, Harris M.** 2005. Hepatitis C virus NS5A-mediated activation of phosphoinositide 3-kinase results in stabilization of cellular beta-catenin and stimulation of beta-catenin-responsive transcription. Journal of virology **79:**5006-5016.

20. **Kumar A, Zloza A, Moon RT, Watts J, Tenorio AR, Al-Harthi L.** 2008. Active beta-catenin signaling is an inhibitory pathway for human immunodeficiency virus replication in peripheral blood mononuclear cells. Journal of virology **82:**2813-2820.

21. **Narasipura SD, Henderson LJ, Fu SW, Chen L, Kashanchi F, Al-Harthi L.** 2012. Role of beta-catenin and TCF/LEF family members in transcriptional activity of HIV in astrocytes. Journal of virology **86:**1911-1921.

22. **Heward JA, Lindsay MA.** 2014. Long non-coding RNAs in the regulation of the immune response. Trends in immunology **35:**408-419.

23. **Khalil AM, Guttman M, Huarte M, Garber M, Raj A, Rivea Morales D, Thomas K, Presser A, Bernstein BE, van Oudenaarden A, Regev A, Lander ES, Rinn JL.** 2009. Many human large intergenic noncoding RNAs associate with chromatin-modifying complexes and affect gene expression. Proceedings of the National Academy of Sciences of the United States of America **106:**11667-11672.

24. **Djebali S, Davis CA, Merkel A, Dobin A, Lassmann T, Mortazavi A, Tanzer A, Lagarde J, Lin W, Schlesinger F, Xue C, Marinov GK, Khatun J, Williams BA, Zaleski C, Rozowsky J, Roder M, Kokocinski F, Abdelhamid RF, Alioto T, Antoshechkin I, Baer MT, Bar NS, Batut P, Bell K, Bell I, Chakrabortty S, Chen X, Chrast J, Curado J, Derrien T, Drenkow J, Dumais E, Dumais J, Duttagupta R, Falconnet E, Fastuca M, Fejes-Toth K, Ferreira P, Foissac S, Fullwood MJ, Gao H, Gonzalez D, Gordon A, Gunawardena H, Howald C, Jha S, Johnson R, Kapranov P, King B, Kingswood C, Luo OJ, Park E, Persaud K, Preall JB, Ribeca P, Risk B, Robyr D, Sammeth M, Schaffer L, See LH, Shahab A, Skancke J, Suzuki AM, Takahashi H, Tilgner H, Trout D, Walters N, Wang H, Wrobel J, Yu Y, Ruan X, Hayashizaki Y, Harrow J, Gerstein M, Hubbard T, Reymond A, Antonarakis SE, Hannon G, Giddings MC, Ruan Y, Wold B, Carninci P, Guigo R, Gingeras TR.** 2012. Landscape of transcription in human cells. Nature **489:**101-108.

25. **Mattick JS.** 2004. RNA regulation: a new genetics? Nature reviews. Genetics **5:**316-323.

26. **Liu Y, Zhang R, Ying K.** 2015. Long noncoding RNAs: novel links in respiratory diseases (review). Molecular medicine reports **11:**4025-4031.

27. **Gupta RA, Shah N, Wang KC, Kim J, Horlings HM, Wong DJ, Tsai MC, Hung T, Argani P, Rinn JL, Wang Y, Brzoska P, Kong B, Li R, West RB, van de Vijver MJ, Sukumar S, Chang HY.** 2010. Long non-coding RNA HOTAIR reprograms chromatin state to promote cancer metastasis. Nature **464:**1071-1076.

28. **Prensner JR, Chinnaiyan AM.** 2011. The emergence of lncRNAs in cancer biology. Cancer discovery **1:**391-407.

29. **Uchida S, Dimmeler S.** 2015. Long noncoding RNAs in cardiovascular diseases. Circulation research **116:**737-750.

30. **Plath K, Mlynarczyk-Evans S, Nusinow DA, Panning B.** 2002. Xist RNA and the mechanism of X chromosome inactivation. Annual review of genetics **36:**233-278.

31. **Martianov I, Ramadass A, Serra Barros A, Chow N, Akoulitchev A.** 2007. Repression of the human dihydrofolate reductase gene by a non-coding interfering transcript. Nature **445:**666-670.

32. **Hung T, Wang Y, Lin MF, Koegel AK, Kotake Y, Grant GD, Horlings HM, Shah N, Umbricht C, Wang P, Wang Y, Kong B, Langerod A, Borresen-Dale AL, Kim SK, van de Vijver M, Sukumar S, Whitfield ML, Kellis M, Xiong Y, Wong DJ, Chang HY.** 2011. Extensive and coordinated transcription of noncoding RNAs within cell-cycle promoters. Nature genetics **43:**621-629.

33. **Poliseno L, Salmena L, Zhang J, Carver B, Haveman WJ, Pandolfi PP.** 2010. A coding-independent function of gene and pseudogene mRNAs regulates tumour biology. Nature **465:**1033-1038.

34. **Bertani S, Sauer S, Bolotin E, Sauer F.** 2011. The noncoding RNA Mistral activates Hoxa6 and Hoxa7 expression and stem cell differentiation by recruiting MLL1 to chromatin. Molecular cell **43:**1040-1046.

35. **Wang KC, Yang YW, Liu B, Sanyal A, Corces-Zimmerman R, Chen Y, Lajoie BR, Protacio A, Flynn RA, Gupta RA, Wysocka J, Lei M, Dekker J, Helms JA, Chang HY.** 2011. A long noncoding RNA maintains active chromatin to coordinate homeotic gene expression. Nature **472:**120-124.

36. **Li Z, Chao TC, Chang KY, Lin N, Patil VS, Shimizu C, Head SR, Burns JC, Rana TM.** 2014. The long noncoding RNA THRIL regulates TNFalpha expression through its interaction with hnRNPL. Proceedings of the National Academy of Sciences of the United States of America **111:**1002-1007.

37. **Rapicavoli NA, Qu K, Zhang J, Mikhail M, Laberge RM, Chang HY.** 2013. A mammalian pseudogene lncRNA at the interface of inflammation and anti-inflammatory therapeutics. eLife **2:**e00762.

38. **Krawczyk M, Emerson BM.** 2014. p50-associated COX-2 extragenic RNA (PACER) activates COX-2 gene expression by occluding repressive NF-kappaB complexes. eLife **3:**e01776.

39. **Carpenter S, Aiello D, Atianand MK, Ricci EP, Gandhi P, Hall LL, Byron M, Monks B, Henry-Bezy M, Lawrence JB, O'Neill LA, Moore MJ, Caffrey DR, Fitzgerald KA.** 2013. A long noncoding RNA mediates both activation and repression of immune response genes. Science (New York, N.Y.) **341:**789-792.

40. **Sharma S, Findlay GM, Bandukwala HS, Oberdoerffer S, Baust B, Li Z, Schmidt V, Hogan PG, Sacks DB, Rao A.** 2011. Dephosphorylation of the nuclear factor of activated T cells (NFAT) transcription factor is regulated by an RNA-protein scaffold complex. Proceedings of the National Academy of Sciences of the United States of America **108:**11381-11386.

41. **Gomez JA, Wapinski OL, Yang YW, Bureau JF, Gopinath S, Monack DM, Chang HY, Brahic M, Kirkegaard K.** 2013. The NeST long ncRNA controls microbial susceptibility and epigenetic activation of the interferon-gamma locus. Cell **152:**743-754.

42. **Liu AY, Torchia BS, Migeon BR, Siliciano RF.** 1997. The human NTT gene: identification of a novel 17-kb noncoding nuclear RNA expressed in activated CD4+ T cells. Genomics **39:**171-184.

43. **Mourtada-Maarabouni M, Hedge VL, Kirkham L, Farzaneh F, Williams GT.** 2008. Growth arrest in human T-cells is controlled by the non-coding RNA growth-arrest-specific transcript 5 (GAS5). Journal of cell science **121:**939-946.

44. **Hu G, Tang Q, Sharma S, Yu F, Escobar TM, Muljo SA, Zhu J, Zhao K.** 2013. Expression and regulation of intergenic long noncoding RNAs during T cell development and differentiation. Nature immunology **14:**1190-1198.

45. **Imam H, Bano AS, Patel P, Holla P, Jameel S.** 2015. The lncRNA NRON modulates HIV-1 replication in a NFAT-dependent manner and is differentially regulated by early and late viral proteins. Scientific reports **5:**8639.

46. **Massimelli MJ, Majerciak V, Kruhlak M, Zheng ZM.** 2013. Interplay between polyadenylate-binding protein 1 and Kaposi's sarcoma-associated herpesvirus ORF57 in accumulation of polyadenylated nuclear RNA, a viral long noncoding RNA. Journal of virology **87:**243-256.

47. **Saayman S, Ackley A, Turner AM, Famiglietti M, Bosque A, Clemson M, Planelles V, Morris KV.** 2014. An HIV-encoded antisense long noncoding RNA epigenetically regulates viral transcription. Molecular therapy : the journal of the American Society of Gene Therapy **22:**1164-1175.

48. **Ouyang J, Zhu X, Chen Y, Wei H, Chen Q, Chi X, Qi B, Zhang L, Zhao Y, Gao GF, Wang G, Chen JL.** 2014. NRAV, a long noncoding RNA, modulates antiviral responses through suppression of interferon-stimulated gene transcription. Cell host & microbe **16:**616-626.

49. **Xiong Y, Jia M, Yuan J, Zhang C, Zhu YAN, Kuang X, Lan LIN, Wang X.** 2015. STAT3-regulated long non-coding RNAs lnc-7SK and lnc-IGF2-AS promote hepatitis C virus replication. Molecular medicine reports **12:**6738-6744.

50. **Winterling C, Koch M, Koeppel M, Garcia-Alcalde F, Karlas A, Meyer TF.** 2014. Evidence for a crucial role of a host non-coding RNA in influenza A virus replication. RNA biology **11:**66-75.

51. **Imamura K, Imamachi N, Akizuki G, Kumakura M, Kawaguchi A, Nagata K, Kato A, Kawaguchi Y, Sato H, Yoneda M, Kai C, Yada T, Suzuki Y, Yamada T, Ozawa T, Kaneki K, Inoue T, Kobayashi M, Kodama T, Wada Y, Sekimizu K, Akimitsu N.** 2014. Long noncoding RNA NEAT1-dependent SFPQ relocation from promoter region to paraspeckle mediates IL8 expression upon immune stimuli. Molecular cell **53:**393-406.

52. **Kambara H, Gunawardane L, Zebrowski E, Kostadinova L, Jobava R, Krokowski D, Hatzoglou M, Anthony DD, Valadkhan S.** 2014. Regulation of Interferon-Stimulated Gene BST2 by a lncRNA Transcribed from a Shared Bidirectional Promoter. Frontiers in immunology **5:**676.

53. **Mishra A, Chintagari NR, Guo Y, Weng T, Su L, Liu L.** 2011. Purinergic P2X7 receptor regulates lung surfactant secretion in a paracrine manner. Journal of cell science **124:**657-668.

54. **Reed L, and Muench H.** 1938. A simple method of estimating fifty percent endpoints. American Journal of Epidemiology **27:**493-497.

55. **Kumar N, Xin Z-t, Liang Y, Ly H, Liang Y.** 2008. NF-κB Signaling Differentially Regulates Influenza Virus RNA Synthesis. Journal of virology **82:**9880-9889.

56. **Shirey KA, Lai W, Scott AJ, Lipsky M, Mistry P, Pletneva LM, Karp CL, McAlees J, Gioannini TL, Weiss J, Chen WH, Ernst RK, Rossignol DP, Gusovsky F, Blanco JC, Vogel SN.** 2013. The TLR4 antagonist Eritoran protects mice from lethal influenza infection. Nature **497:**498-502.

57. **Perwitasari O, Johnson S, Yan X, Howerth E, Shacham S, Landesman Y, Baloglu E, McCauley D, Tamir S, Tompkins SM, Tripp RA.** 2014. Verdinexor, a novel selective inhibitor of nuclear export, reduces influenza a virus replication in vitro and in vivo. Journal of virology **88:**10228-10243.

58. **Huang C, Yang Y, Liu L.** 2015. Interaction of long noncoding RNAs and microRNAs in the pathogenesis of idiopathic pulmonary fibrosis. Physiological genomics **47:**463-469.

59. **Samji T.** 2009. Influenza A: Understanding the Viral Life Cycle. The Yale Journal of Biology and Medicine **82:**153-159.

60. **Lamb RA, and R. M. Krug.** 2003. Orthomyxoviridae: the viruses and their replication, 4 ed, vol. 2. Lippincott-Raven Publishers, Philadelphia, PA.

61. **Wray SK, Gilbert BE, Noall MW, Knight V.** 1985. Mode of action of ribavirin: effect of nucleotide pool alterations on influenza virus ribonucleoprotein synthesis. Antiviral research **5:**29-37.

62. **Garcia-Sastre A.** 2011. Induction and evasion of type I interferon responses by influenza viruses. Virus research **162:**12-18.

63. **Juang YT, Lowther W, Kellum M, Au WC, Lin R, Hiscott J, Pitha PM.** 1998. Primary activation of interferon A and interferon B gene transcription by interferon regulatory factor 3. Proceedings of the National Academy of Sciences of the United States of America **95:**9837-9842.

64. **Emeny JM, Morgan MJ.** 1979. Regulation of the interferon system: evidence that Vero cells have a genetic defect in interferon production. The Journal of general virology **43:**247-252.

65. **Wang J, Edeen K, Manzer R, Chang Y, Wang S, Chen X, Funk CJ, Cosgrove GP, Fang X, Mason RJ.** 2007. Differentiated human alveolar epithelial cells and reversibility of their phenotype in vitro. American journal of respiratory cell and molecular biology **36:**661-668.

66. **Bhaskaran M, Kolliputi N, Wang Y, Gou D, Chintagari NR, Liu L.** 2007. Trans-differentiation of alveolar epithelial type II cells to type I cells involves autocrine signaling by transforming growth factor beta 1 through the Smad pathway. The Journal of biological chemistry **282:**3968-3976.

67. **Arias-Romero LE, Villamar-Cruz O, Huang M, Hoeflich KP, Chernoff J.** 2013. Pak1 kinase links ErbB2 to beta-catenin in transformation of breast epithelial cells. Cancer research **73:**3671-3682.

68. **Matute-Bello G, Downey G, Moore BB, Groshong SD, Matthay MA, Slutsky AS, Kuebler WM.** 2011. An official American Thoracic Society workshop report: features and measurements of experimental acute lung injury in animals. American journal of respiratory cell and molecular biology **44:**725-738.

69. **Westall GP, Paraskeva M.** 2011. H1N1 influenza: critical care aspects. Seminars in respiratory and critical care medicine **32:**400-408.

70. **Buggele WA, Johnson KE, Horvath CM.** 2012. Influenza A virus infection of human respiratory cells induces primary microRNA expression. The Journal of biological chemistry **287:**31027-31040.

71. **Sadler AJ, Williams BR.** 2008. Interferon-inducible antiviral effectors. Nature reviews. Immunology **8:**559-568.

72. **Villegas VE, Zaphiropoulos PG.** 2015. Neighboring gene regulation by antisense long non-coding RNAs. International journal of molecular sciences **16:**3251-3266.

73. **Hassan IH, Zhang MS, Powers LS, Shao JQ, Baltrusaitis J, Rutkowski DT, Legge K, Monick MM.** 2012. Influenza A viral replication is blocked by inhibition of the inositol-requiring enzyme 1 (IRE1) stress pathway. The Journal of biological chemistry **287:**4679-4689.

74. **Roberson EC, Tully JE, Guala AS, Reiss JN, Godburn KE, Pociask DA, Alcorn JF, Riches DW, Dienz O, Janssen-Heininger YM, Anathy V.** 2012. Influenza induces endoplasmic reticulum stress, caspase-12-dependent apoptosis, and c-Jun N-terminal kinase-mediated transforming growth factor-beta release in lung epithelial cells. American journal of respiratory cell and molecular biology **46:**573-581.

75. **Dittmann J, Stertz S, Grimm D, Steel J, Garcia-Sastre A, Haller O, Kochs G.** 2008. Influenza A virus strains differ in sensitivity to the antiviral action of Mx-GTPase. Journal of virology **82:**3624-3631.

76. **Melchjorsen J, Kristiansen H, Christiansen R, Rintahaka J, Matikainen S, Paludan SR, Hartmann R.** 2009. Differential regulation of the OASL and OAS1 genes in response to viral infections. Journal of interferon & cytokine research : the official journal of the International Society for Interferon and Cytokine Research **29:**199-207.

77. **Lankat-Buttgereit B, Tampe R.** 2002. The transporter associated with antigen processing: function and implications in human diseases. Physiological reviews **82:**187-204.

78. **Huang CH, Tanaka Y, Fujito NT, Nonaka M.** 2013. Dimorphisms of the proteasome subunit beta type 8 gene (PSMB8) of ectothermic tetrapods originated in multiple independent evolutionary events. Immunogenetics **65:**811-821.

79. **Nimmerjahn F, Dudziak D, Dirmeier U, Hobom G, Riedel A, Schlee M, Staudt LM, Rosenwald A, Behrends U, Bornkamm GW, Mautner J.** 2004. Active NF-kappaB signalling is a prerequisite for influenza virus infection. The Journal of general virology **85:**2347-2356.

80. **Wurzer WJ, Ehrhardt C, Pleschka S, Berberich-Siebelt F, Wolff T, Walczak H, Planz O, Ludwig S.** 2004. NF-kappaB-dependent induction of tumor necrosis factor-related apoptosis-inducing ligand (TRAIL) and Fas/FasL is crucial for efficient influenza virus propagation. The Journal of biological chemistry **279:**30931-30937.

81. **Pleschka S, Wolff T, Ehrhardt C, Hobom G, Planz O, Rapp UR, Ludwig S.** 2001. Influenza virus propagation is impaired by inhibition of the Raf/MEK/ERK signalling cascade. Nature cell biology **3:**301-305.

82. **Hale BG, Jackson D, Chen YH, Lamb RA, Randall RE.** 2006. Influenza A virus NS1 protein binds p85beta and activates phosphatidylinositol-3-kinase signaling. Proceedings of the National Academy of Sciences of the United States of America **103:**14194-14199.

83. **Lu Y, Wambach M, Katze MG, Krug RM.** 1995. Binding of the influenza virus NS1 protein to double-stranded RNA inhibits the activation of the protein kinase that phosphorylates the elF-2 translation initiation factor. Virology **214:**222-228.

84. **Akira S, Uematsu S, Takeuchi O.** 2006. Pathogen recognition and innate immunity. Cell **124:**783-801.

85. **Gack MU, Albrecht RA, Urano T, Inn KS, Huang IC, Carnero E, Farzan M, Inoue S, Jung JU, Garcia-Sastre A.** 2009. Influenza A virus NS1 targets the ubiquitin ligase TRIM25 to evade recognition by the host viral RNA sensor RIG-I. Cell host & microbe **5:**439-449.

86. **Hillesheim A, Nordhoff C, Boergeling Y, Ludwig S, Wixler V.** 2014. beta-catenin promotes the type I IFN synthesis and the IFN-dependent signaling response but is suppressed by influenza A virus-induced RIG-I/NF-kappaB signaling. Cell communication and signaling : CCS **12:**29.

87. **Baril M, Es-Saad S, Chatel-Chaix L, Fink K, Pham T, Raymond VA, Audette K, Guenier AS, Duchaine J, Servant M, Bilodeau M, Cohen E, Grandvaux N, Lamarre D.** 2013. Genome-wide RNAi screen reveals a new role of a WNT/CTNNB1 signaling pathway as negative regulator of virus-induced innate immune responses. PLoS pathogens **9:**e1003416.

88. **Tanaka M, Yamazaki Y, Kanno Y, Igarashi K, Aisaki K-i, Kanno J, Nakamura T.** 2014. Ewing's sarcoma precursors are highly enriched in embryonic osteochondrogenic progenitors. The Journal of Clinical Investigation **124:**3061-3074.

89. **Govorkova EA, Webster RG.** 2010. Combination chemotherapy for influenza. Viruses **2:**1510-1529.

90. **Benitez AA, Panis M, Xue J, Varble A, Shim JV, Frick AL, Lopez CB, Sachs D, tenOever BR.** 2015. In Vivo RNAi Screening Identifies MDA5 as a Significant Contributor to the Cellular Defense against Influenza A Virus. Cell reports **11:**1714-1726.

91. **Cheng H, Koning K, O'Hearn A, Wang M, Rumschlag-Booms E, Varhegyi E, Rong L.** 2015. A parallel genome-wide RNAi screening strategy to identify host proteins important for entry of Marburg virus and H5N1 influenza virus. Virology journal **12:**194.

92. **Wilk E, Pandey AK, Leist SR, Hatesuer B, Preusse M, Pommerenke C, Wang J, Schughart K.** 2015. RNAseq expression analysis of resistant and susceptible mice after influenza A virus infection identifies novel genes associated with virus replication and important for host resistance to infection. BMC genomics **16:**655.

93. **Garfinkel MS, Katze MG.** 1993. Translational control by influenza virus. Selective translation is mediated by sequences within the viral mRNA 5'-untranslated region. The Journal of biological chemistry **268:**22223-22226.

94. **Li J, Hou R, Niu X, Liu R, Wang Q, Wang C, Li X, Hao Z, Yin G, Zhang K.** 2016. Comparison of microarray and RNA-Seq analysis of mRNA expression in dermal mesenchymal stem cells. Biotechnology letters **38:**33-41.

95. **Inglis SC.** 1982. Inhibition of host protein synthesis and degradation of cellular mRNAs during infection by influenza and herpes simplex virus. Molecular and cellular biology **2:**1644-1648.

96. **Beloso A, Martinez C, Valcarcel J, Santaren JF, Ortin J.** 1992. Degradation of cellular mRNA during influenza virus infection: its possible role in protein synthesis shutoff. The Journal of general virology **73 (Pt 3):**575-581.

97. **Lakadamyali M, Rust MJ, Zhuang X.** 2004. Endocytosis of influenza viruses. Microbes and infection / Institut Pasteur **6:**929-936.

98. **Josset L, Tchitchek N, Gralinski LE, Ferris MT, Eisfeld AJ, Green RR, Thomas MJ, Tisoncik-Go J, Schroth GP, Kawaoka Y, Pardo-Manuel de Villena F, Baric RS, Heise MT, Peng X, Katze MG.** 2014. Annotation of long non-coding RNAs expressed

in Collaborative Cross founder mice in response to respiratory virus infection reveals a new class of interferon-stimulated transcripts. RNA biology **11:**875-890.

99. **Kambara H, Niazi F, Kostadinova L, Moonka DK, Siegel CT, Post AB, Carnero E, Barriocanal M, Fortes P, Anthony DD, Valadkhan S.** 2014. Negative regulation of the interferon response by an interferon-induced long non-coding RNA. Nucleic acids research **42:**10668-10680.

100. **Winterling C, Koch M, Koeppel M, Garcia-Alcalde F, Karlas A, Meyer TF.** 2014. Evidence for a crucial role of a host non-coding RNA in influenza A virus replication. RNA biology **11:**66-75.

101. **Yuan SX, Wang J, Yang F, Tao QF, Zhang J, Wang LL, Yang Y, Liu H, Wang ZG, Xu QG, Fan J, Liu L, Sun SH, Zhou WP.** 2016. Long noncoding RNA DANCR increases stemness features of hepatocellular carcinoma by derepression of CTNNB1. Hepatology (Baltimore, Md.) **63:**499-511.

102. **Nakagawa S, Kageyama Y.** 2014. Nuclear lncRNAs as epigenetic regulators-beyond skepticism. Biochimica et biophysica acta **1839:**215-222.

103. **Nakagawa S, Ip JY, Shioi G, Tripathi V, Zong X, Hirose T, Prasanth KV.** 2012. Malat1 is not an essential component of nuclear speckles in mice. RNA (New York, N.Y.) **18:**1487-1499.

104. **Clemson CM, Hutchinson JN, Sara SA, Ensminger AW, Fox AH, Chess A, Lawrence JB.** 2009. An architectural role for a nuclear noncoding RNA: NEAT1 RNA is essential for the structure of paraspeckles. Molecular cell **33:**717-726.

105. **Gutschner T, Hammerle M, Eissmann M, Hsu J, Kim Y, Hung G, Revenko A, Arun G, Stentrup M, Gross M, Zornig M, MacLeod AR, Spector DL, Diederichs S.** 2013.

The noncoding RNA MALAT1 is a critical regulator of the metastasis phenotype of lung cancer cells. Cancer research **73:**1180-1189.

106. **Zhang K, Shi ZM, Chang YN, Hu ZM, Qi HX, Hong W.** 2014. The ways of action of long non-coding RNAs in cytoplasm and nucleus. Gene **547:**1-9.

107. **Ho AW, Prabhu N, Betts RJ, Ge MQ, Dai X, Hutchinson PE, Lew FC, Wong KL, Hanson BJ, Macary PA, Kemeny DM.** 2011. Lung CD103+ dendritic cells efficiently transport influenza virus to the lymph node and load viral antigen onto MHC class I for presentation to CD8 T cells. Journal of immunology (Baltimore, Md. : 1950) **187:**6011-6021.

108. **Go JT, Belisle SE, Tchitchek N, Tumpey TM, Ma W, Richt JA, Safronetz D, Feldmann H, Katze MG.** 2012. 2009 pandemic H1N1 influenza virus elicits similar clinical course but differential host transcriptional response in mouse, macaque, and swine infection models. BMC genomics **13:**627.

109. **Bordignon J, Probst CM, Mosimann AL, Pavoni DP, Stella V, Buck GA, Satproedprai N, Fawcett P, Zanata SM, de Noronha L, Krieger MA, Duarte Dos Santos CN.** 2008. Expression profile of interferon stimulated genes in central nervous system of mice infected with dengue virus Type-1. Virology **377:**319-329.

110. **Flori L, Rogel-Gaillard C, Cochet M, Lemonnier G, Hugot K, Chardon P, Robin S, Lefevre F.** 2008. Transcriptomic analysis of the dialogue between Pseudorabies virus and porcine epithelial cells during infection. BMC genomics **9:**123.

111. **Neville LF, Mathiak G, Bagasra O.** 1997. The immunobiology of interferon-gamma inducible protein 10 kD (IP-10): a novel, pleiotropic member of the C-X-C chemokine superfamily. Cytokine & growth factor reviews **8:**207-219.

112. **Ichikawa A, Kuba K, Morita M, Chida S, Tezuka H, Hara H, Sasaki T, Ohteki T, Ranieri VM, dos Santos CC, Kawaoka Y, Akira S, Luster AD, Lu B, Penninger JM, Uhlig S, Slutsky AS, Imai Y.** 2013. CXCL10-CXCR3 enhances the development of neutrophil-mediated fulminant lung injury of viral and nonviral origin. American journal of respiratory and critical care medicine **187:**65-77.

113. **Tang NL, Chan PK, Wong CK, To KF, Wu AK, Sung YM, Hui DS, Sung JJ, Lam CW.** 2005. Early enhanced expression of interferon-inducible protein-10 (CXCL-10) and other chemokines predicts adverse outcome in severe acute respiratory syndrome. Clinical chemistry **51:**2333-2340.

114. **Chan MC, Kuok DI, Leung CY, Hui KP, Valkenburg SA, Lau EH, Nicholls JM, Fang X, Guan Y, Lee JW, Chan RW, Webster RG, Matthay MA, Peiris JS.** 2016. Human mesenchymal stromal cells reduce influenza A H5N1-associated acute lung injury in vitro and in vivo. Proceedings of the National Academy of Sciences of the United States of America.

115. **Oslund KL, Zhou X, Lee B, Zhu L, Duong T, Shih R, Baumgarth N, Hung L-Y, Wu R, Chen Y.** 2014. Synergistic Up-Regulation of CXCL10 by Virus and IFN γ in Human Airway Epithelial Cells. PloS one **9:**e100978.

116. **Sauty A, Dziejman M, Taha RA, Iarossi AS, Neote K, Garcia-Zepeda EA, Hamid Q, Luster AD.** 1999. The T cell-specific CXC chemokines IP-10, Mig, and I-TAC are expressed by activated human bronchial epithelial cells. Journal of immunology (Baltimore, Md. : 1950) **162:**3549-3558.

117. **Wu W, Zhang W, Booth JL, Metcalf JP.** 2012. Influenza A(H1N1)pdm09 virus suppresses RIG-I initiated innate antiviral responses in the human lung. PloS one **7:**e49856.

118. **Tisoncik JR, Korth MJ, Simmons CP, Farrar J, Martin TR, Katze MG.** 2012. Into the eye of the cytokine storm. Microbiology and molecular biology reviews : MMBR **76:**16-32.

119. **Wang W, Yang P, Zhong Y, Zhao Z, Xing L, Zhao Y, Zou Z, Zhang Y, Li C, Li T, Wang C, Wang Z, Yu X, Cao B, Gao X, Penninger JM, Wang X, Jiang C.** 2013. Monoclonal antibody against CXCL-10/IP-10 ameliorates influenza A (H1N1) virus induced acute lung injury. Cell research **23:**577-580.

120. **Falconer K, Askarieh G, Weis N, Hellstrand K, Alaeus A, Lagging M.** 2010. IP-10 predicts the first phase decline of HCV RNA and overall viral response to therapy in patients co-infected with chronic hepatitis C virus infection and HIV. Scandinavian journal of infectious diseases **42:**896-901.

121. **Lane BR, King SR, Bock PJ, Strieter RM, Coffey MJ, Markovitz DM.** 2003. The C-X-C chemokine IP-10 stimulates HIV-1 replication. Virology **307:**122-134.

VITA

SUNIL MORE

Candidate for the Degree of

Doctor of Philosophy

Thesis: IDENTIFICATION OF HOST FACTORS FOR DEVELOPING ANTIVIRAL STRATEGIES AGAINST INFLUENZA VIRUS

Major Field: Veterinary Biomedical Science

Biographical:

Education:

Completed the requirements for the Doctor of Philosophy in Veterinary Biomedical Sciences at Oklahoma State University, Stillwater, Oklahoma in May, 2016.

Completed the requirements for the Master of Veterinary Science in Animal Genetics at Maharashtra Animal and Fishery Sciences University, Nagpur, Maharashtra/India in 2009.

Completed the requirements for the Bachelor of Veterinary Science in Veterinary Medicine at Maharashtra Animal and Fishery Sciences University, Nagpur, Maharashtra/India in 2007.

Experience:
Graduate Teaching Associate: 2010 – 2014
Graduate Research Associate: 2010 – 2016

Professional Memberships:
American Association for Advancement of Science